

- **ВЛИЯНИЕ ОРБИТАЛЬНЫХ СТЕПЕНЕЙ СВОБОДЫ
ЭЛЕКТРОНА НА МАГНИТОТРАНСПОРТ В
ПОЛУПРОВОДНИКАХ**

- Аплеснин С.С., Романова О.Б., Ситников М.Н., Королев В.В.,
Кретинин В.В.

-

- ¹Kirensky Institute of Physics, RAS, 660036, Krasnoyarsk, Russia
- ²Department of Physics, Siberian State Aerospace University, 660014,
Krasnoyarsk, Russia

Motivation

Searching and research of materials for spintronics on the basis of a magnetoresistance is an actual task. The materials revealed magnetoresistance in paramagnetic state in the room temperatures are interest.

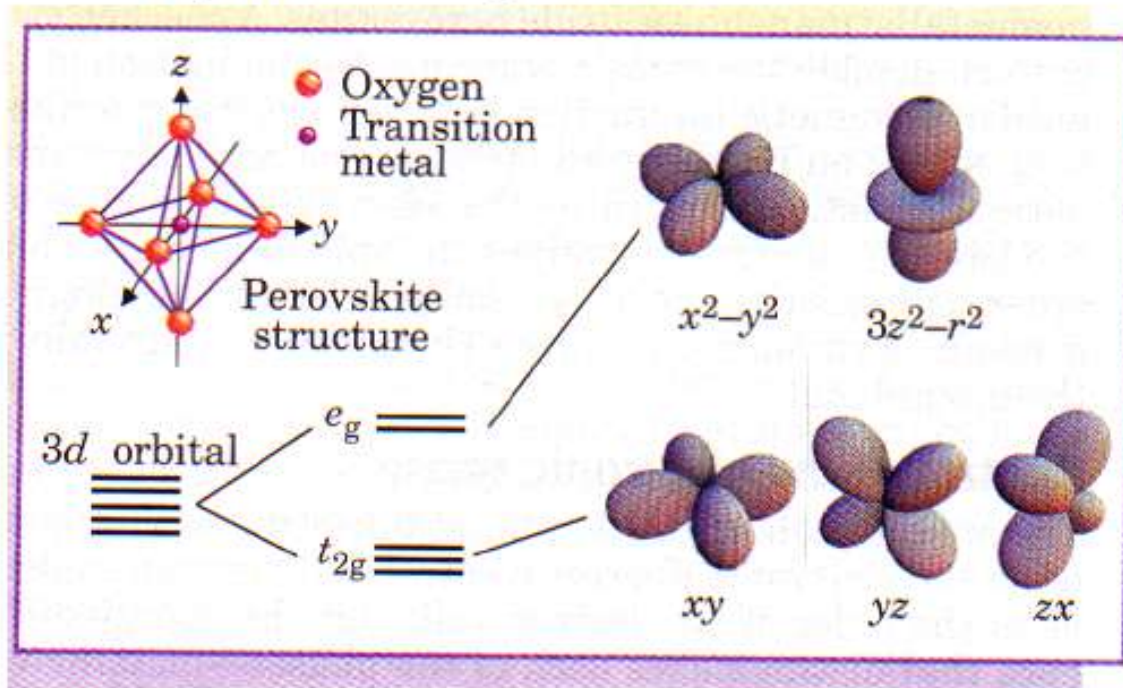
The electronic doping of manganese sulfides in results of substitution of rare-earth ions with variable valance can induce spin, charging and orbital ordering with close relationship between them. Magnetic properties can change under electric field and dielectric properties under pressure.

Outline

1. Magnetoresistance in non-magnetic compounds and paramagnetic state
2. Resistance and I-U dependence of $Tm_xMn_{1-x}S$ versus magnetic field
3. Magnetoimpedance and magnetocapacity
4. Polarization and pyrocurrent
5. Magnetic properties of $Tm_xMn_{1-x}S$

Partially the filled t_{2g}-level of d¹ (Ti³⁺, V⁴⁺), d² (Ti²⁺, V³⁺, Cr⁴⁺) ions in an octahedral environment

3- d ион в кристаллическом поле кубической решетки

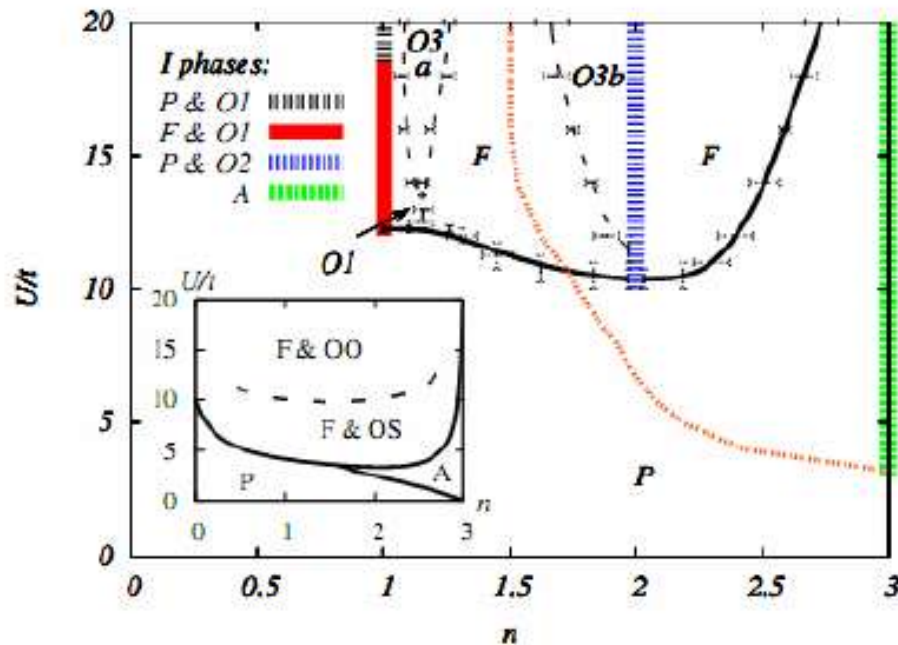
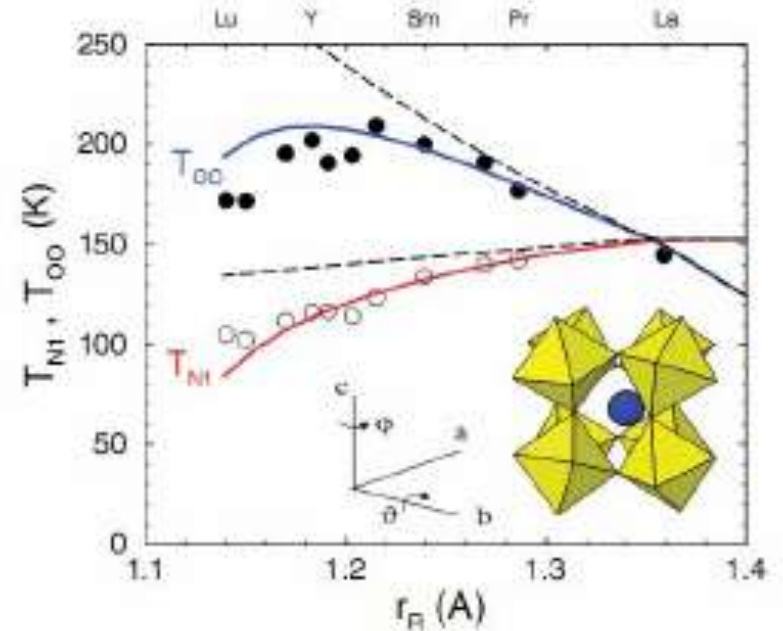
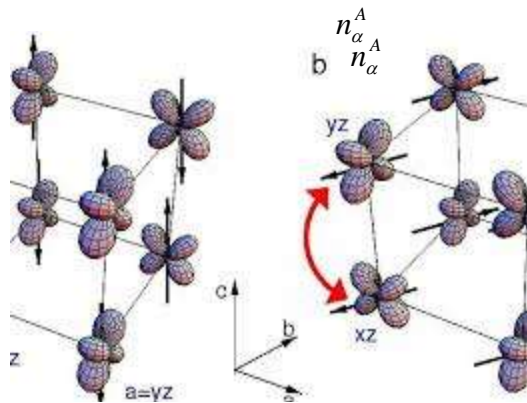


$$\frac{1}{\sqrt{2}} (|yz\rangle \pm |zx\rangle)$$

Orbital ordering: AFM, FM, incommensurate

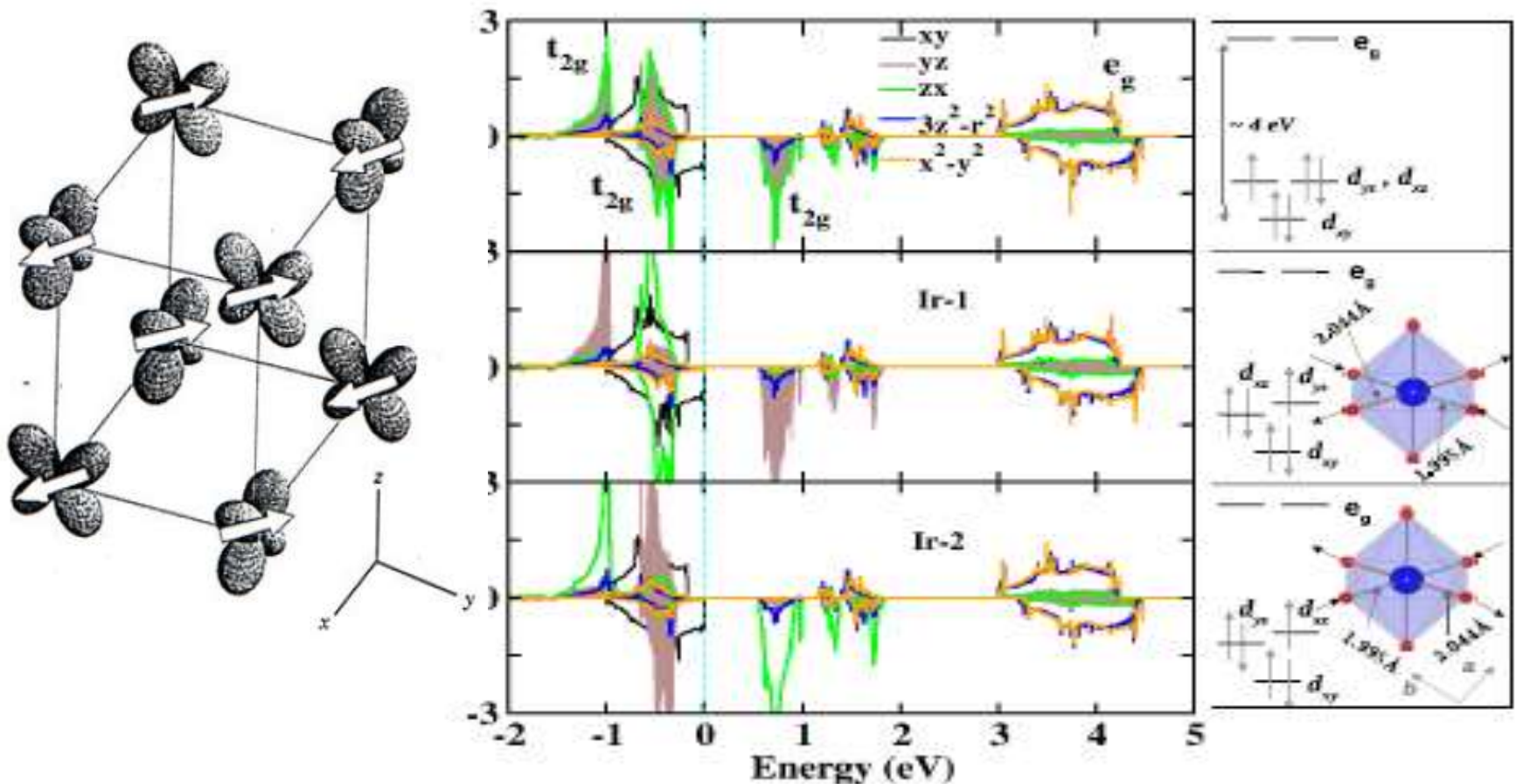
J.-S. Zhou et al PRL, 2007, v. 99, p. 156401

ReVO₃, KCuCl₃

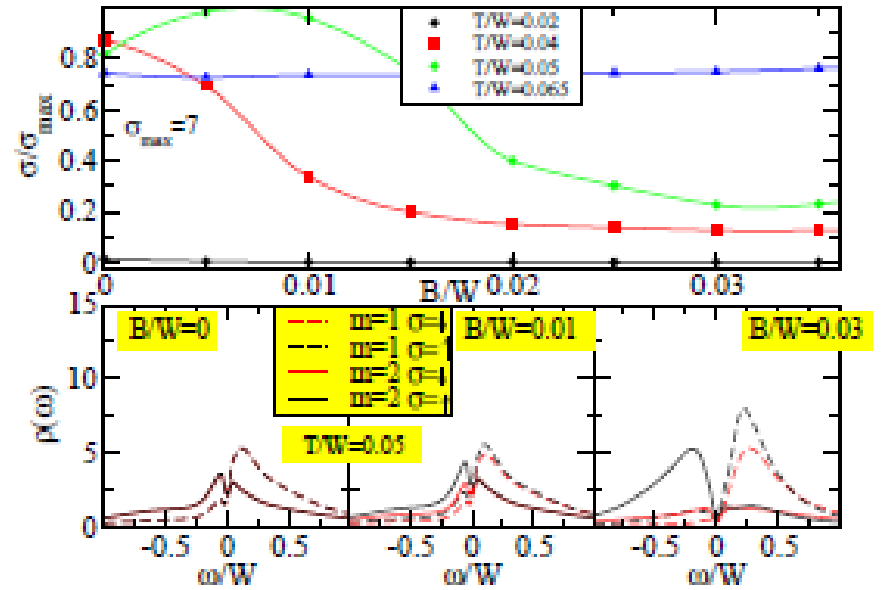
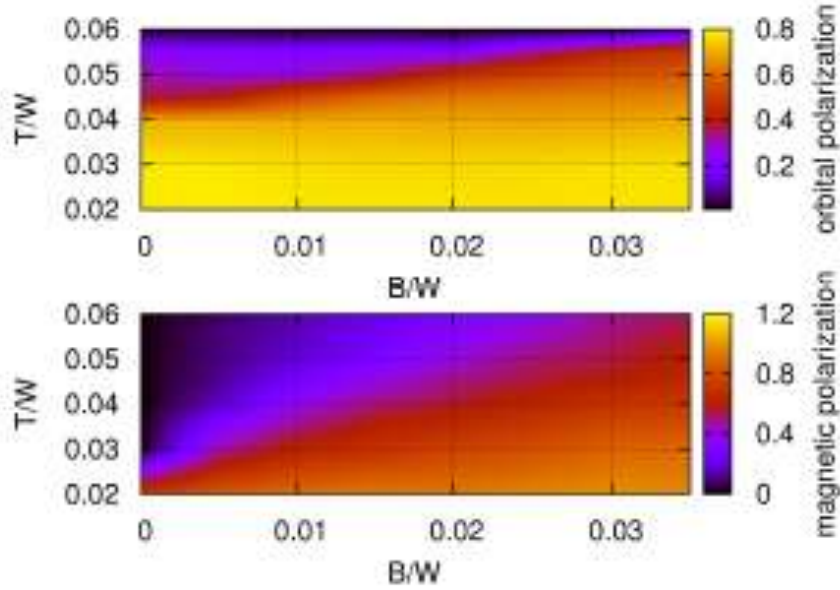


$(n_\alpha^A, n_\beta^A, n_\chi^A \mid n_\alpha^B, n_\beta^B, n_\chi^B)$	
$(1-\delta, \delta, \delta \mid \delta, \frac{1}{2}, \frac{1}{2})$	$(\uparrow\uparrow\uparrow \mid \uparrow\uparrow\uparrow)$
$(\frac{1}{2}, \frac{1}{2}, 1 \mid 1, 1, 0)$	$(\uparrow\uparrow\uparrow \mid \uparrow\uparrow 0)$
$(1-2\delta, 2\delta, \delta \mid \delta, 2\delta, 1-2\delta)$	$(\uparrow\uparrow\uparrow \mid \uparrow\uparrow\uparrow)$
$(2\delta, 1-2\delta, 1-\delta \mid 1-\delta, 1-2\delta, 2\delta)$	$(\uparrow\uparrow\uparrow \mid \uparrow\uparrow\uparrow)$

- Electron structure Sr₂CeIrO₆ with Ir⁴ (5d⁵, S=1/2) with AFM d_{yz} и d_{xz} orbital and two bond length . The experimental band gap (≈ 0.3 eV) agrees qualitatively with the Ir eff GGA+U+SOC (U eV) AFM band gap (≈ 0.35 eV) .
Martin Jansen,* arXiv:1507.08682v1



Change of resistance in a magnetic field upon transition to an orbital-ordered state. Robert Peters* and Norio Kawakami PRL 117, 076801 (2011)



$$\begin{aligned}
 H &= H_T + H_U \\
 H_T &= \sum_{\langle i,j \rangle, \sigma, m} t_{i,j} c_{i,\sigma,m}^\dagger c_{j,\sigma,m} \quad \tilde{U}/W = 4, \\
 H_U &= \sum_i \left(\sum_m U n_{i,\uparrow,m} n_{i,\downarrow,m} \right. \\
 &\quad \left. + \left(U' - \frac{J}{2} \right) (n_{i,\uparrow,0} + n_{i,\downarrow,0}) (n_{i,\uparrow,1} + n_{i,\downarrow,1}) \right. \\
 &\quad \left. - 2J \vec{S}_{i,0} \cdot \vec{S}_{i,1} \right),
 \end{aligned}$$

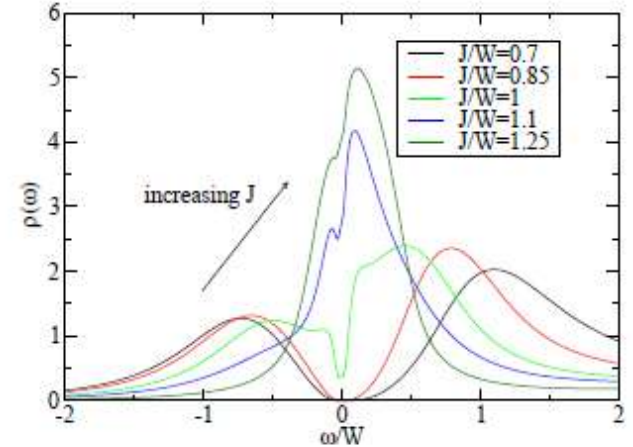


Figure 5. (color online) Spectral functions for $U = 4W$, $T/W = 0.08$, $U' = U - 2J$, and different J . For all shown spectral functions the system is in a paramagnetic state. For

Топологические изоляторы

$$H_{so} = \frac{\alpha_R}{\hbar} \vec{e}_z [\vec{\sigma} \times (\vec{p} - e\vec{A})].$$

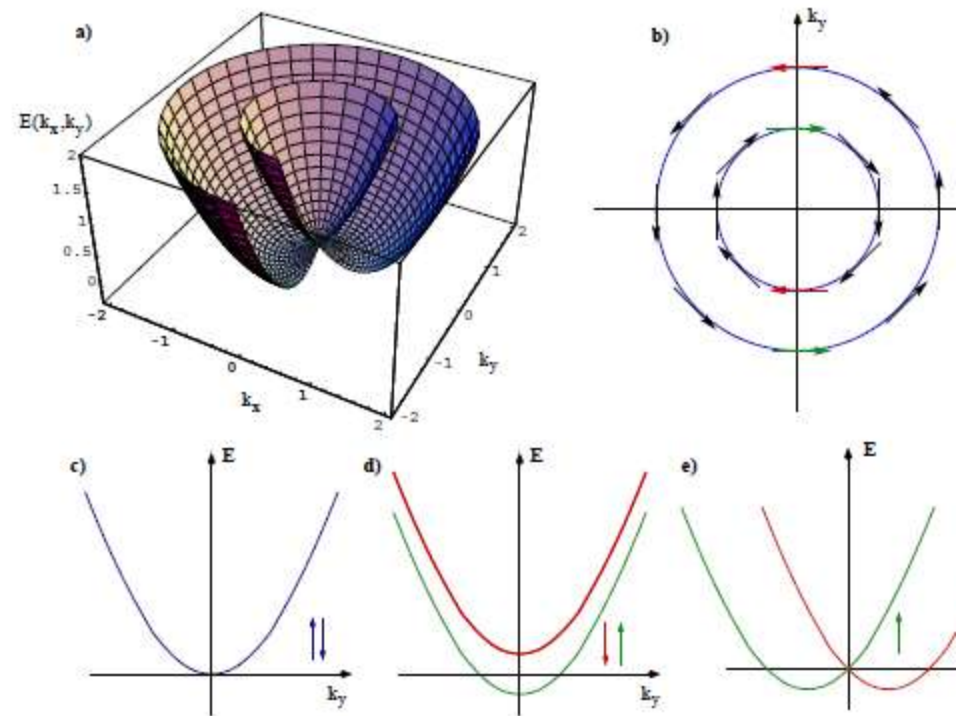
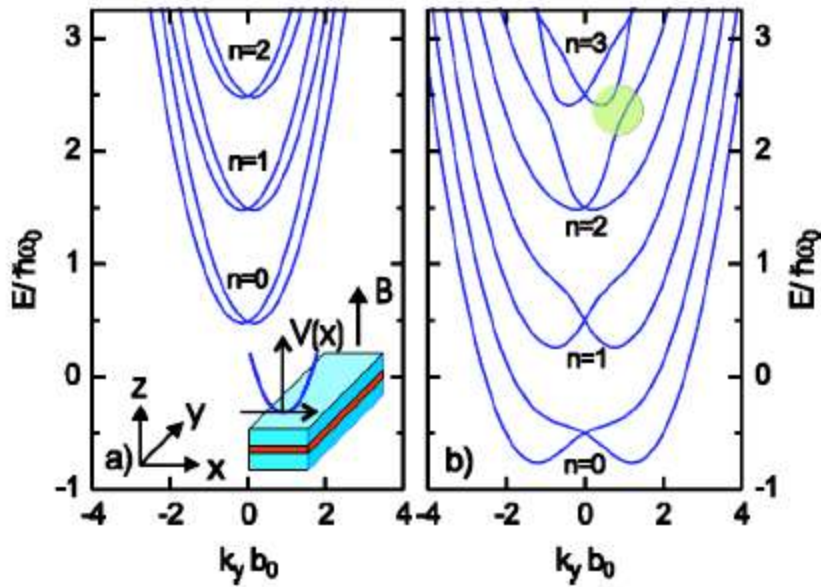
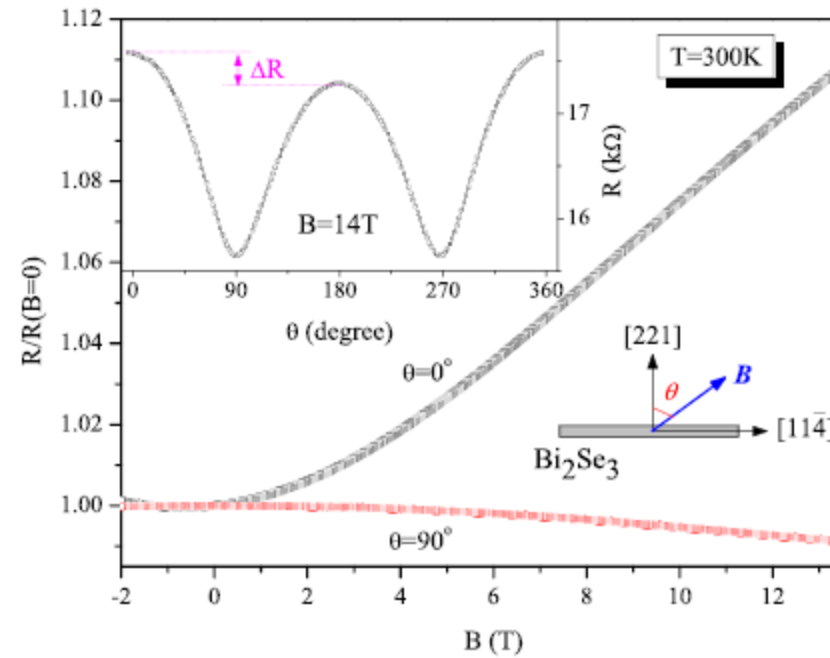
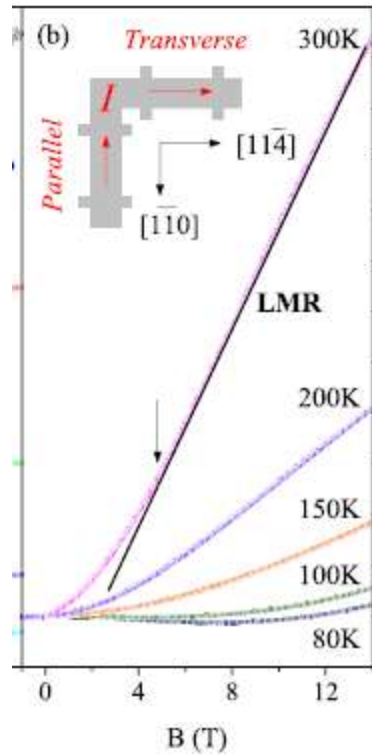
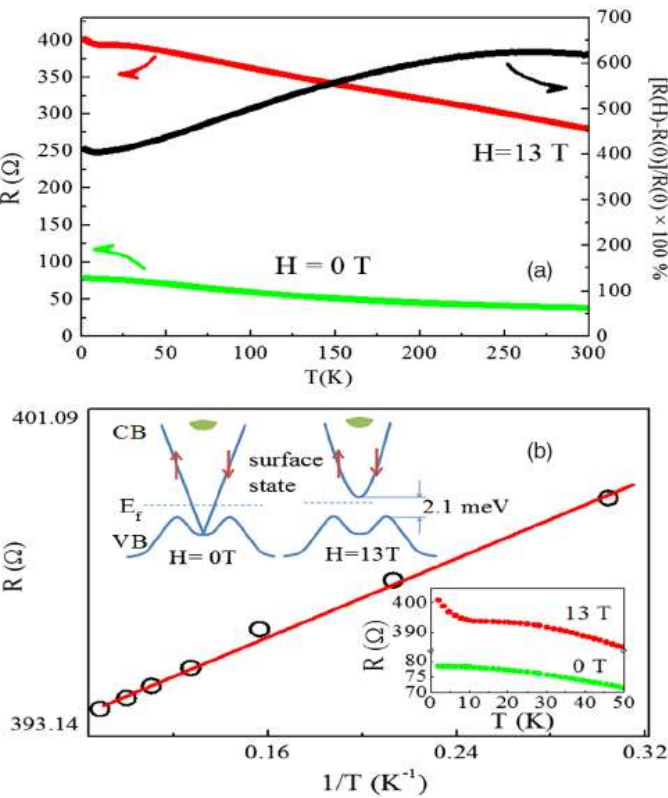


FIG. 1. (Color online) Energy dispersion of the spin-split subbands at $B=0$ for weak spin-orbit coupling: $\Delta_{so}/\hbar\omega_0=0.01$ (a) and for strong spin-orbit coupling for $\Delta_{so}/\hbar\omega_0=1$ (b). The anticrossing

$$\mathcal{E}_{\pm}(\vec{k}) = \frac{\hbar^2 k^2}{2m} \pm \alpha k = \frac{\hbar^2}{2m} (k \pm k_{SO})^2 - \Delta_{SO},$$

Магнитосопротивление в топологических изоляторах



Appl. Phys. Lett. 103, 031606 (2013)

FIG. 2 (color online). (a) Temperature dependence of the resistance and magnetoresistance of a Bi_2Te_3 nanosheet.

(b) Anisotropic plot of $R/R(0)$ vs $1/T$ for low temperatures. Upper: Xiaolin Wang PRL 108, 266806 (2012)

Уровни Ландау в магнитном поле

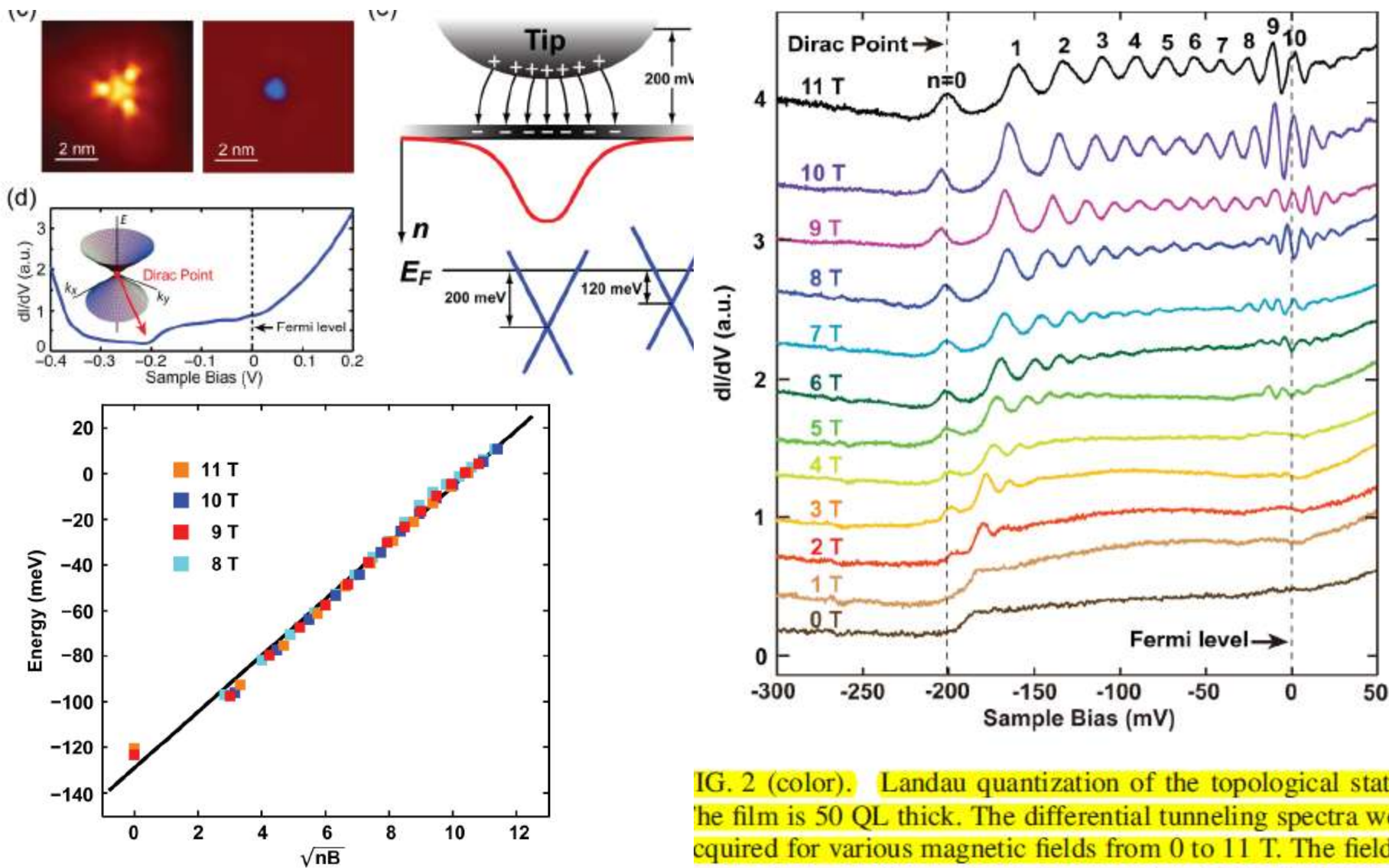


FIG. 2 (color). Landau quantization of the topological states. The film is 50 QL thick. The differential tunneling spectra were acquired for various magnetic fields from 0 to 11 T. The field is

$$E_n = E_D^0 + \text{sgn}(n)v_F\sqrt{2eB\hbar|n|}, \quad n = 0, \pm 1, \pm 2, \dots,$$

Вычисление магнитосопротивления в модели со спин-орбитальным взаимодействием

$$H = v_F ((p + eA) \times \sigma) \cdot z + V(x, y)$$

$$J = \frac{e}{h} \int dE T_{LR}(E) [f_L(E) - f_R(E)]$$

$$T_{LR}(E) = \text{Tr} [\Gamma_L G^r \Gamma_R G^a]$$

Current injection

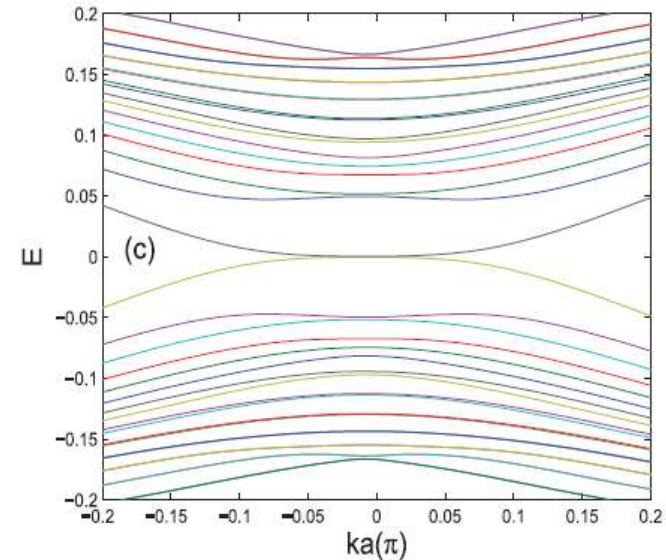
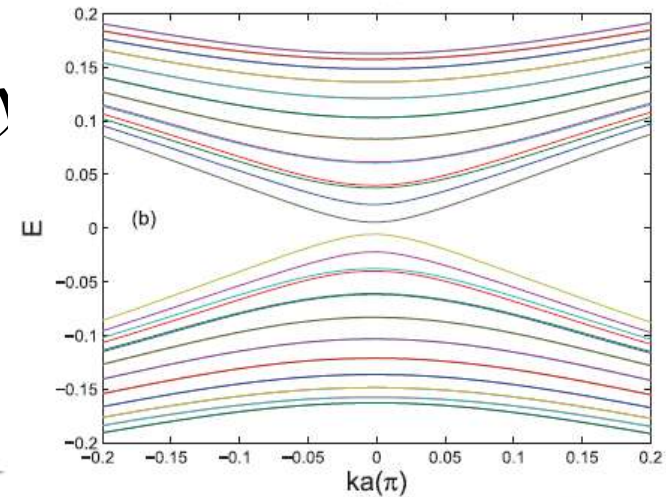
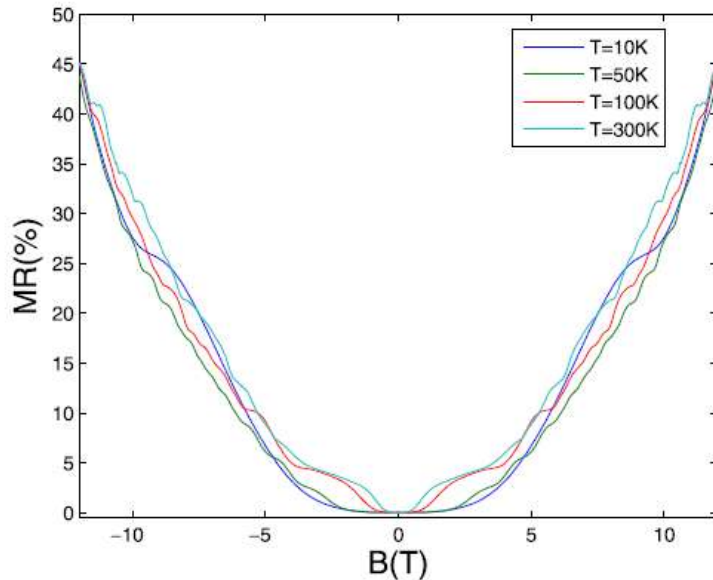
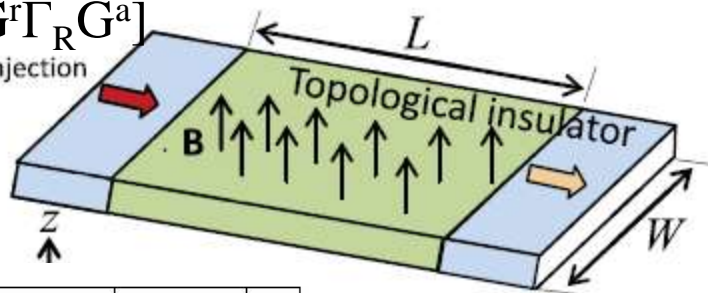


Fig. 2. Energy band structure of the TI waveguide confined in the y-direction for the cases (a) $B=0$, (b) $B=2$ T, and (c) $B=8$ T. The lattice constant a is 0.35 nm, the length L is 60 nm and the width W is 40 nm, and the Fermi velocity is chosen as 5.0×10^5 m/s.

Electrical-field induced giant magnetoresistivity in (non-magnetic) phase change films

Junji Tominaga, APPLIED PHYSICS LETTERS 99, 152105 (2011)

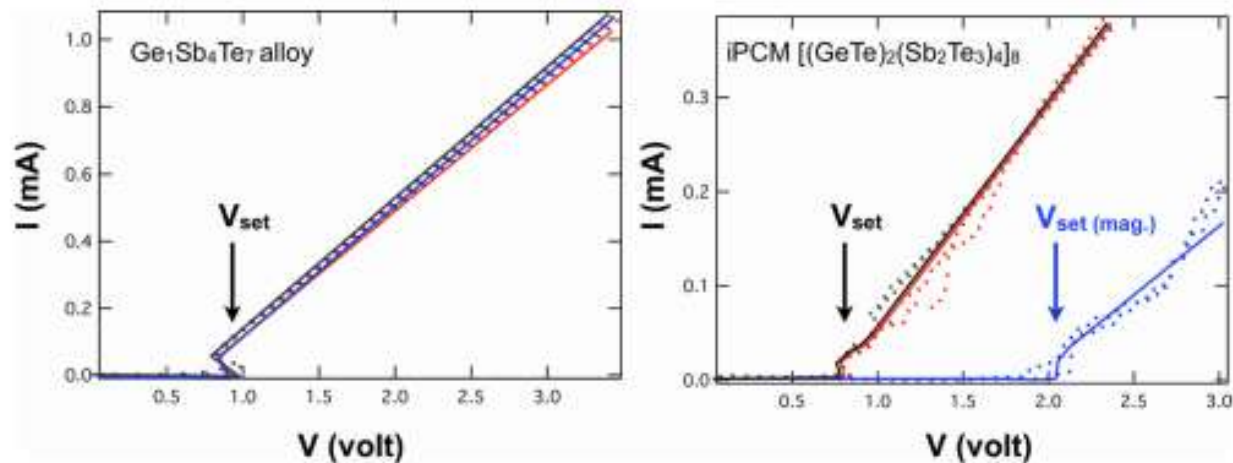


FIG. 2. (Color online) Current-Voltage characteristics of a PCRAM device fabricated using composite $\text{Ge}_1\text{Sb}_4\text{Te}_7$ (left) and an identical composition iPCM device (right). As the voltage reaches the threshold value of V_{set} , the device switches into the low-resistance state. Device characteristics prior to application of a magnetic field, with an external magnetic field of 0.1 T applied, and after removal of the field are shown. The composite device (left) did not show any change among the three states, while the iPCM device (right) clearly showed a voltage shift under the magnetic field, indicated as $V_{\text{set}}(\text{mag.})$. A sequence of 300 ns pulses was used for the measurements. Two scans for each state are shown to demonstrate reproducibility. Dots are experimental data and solid lines are guides for the eye.

Non-saturating magnetoresistance in heavily disordered semiconductors M.M. Parish, P.B. Littlewood. *Nature*, 426, 162 (2003)

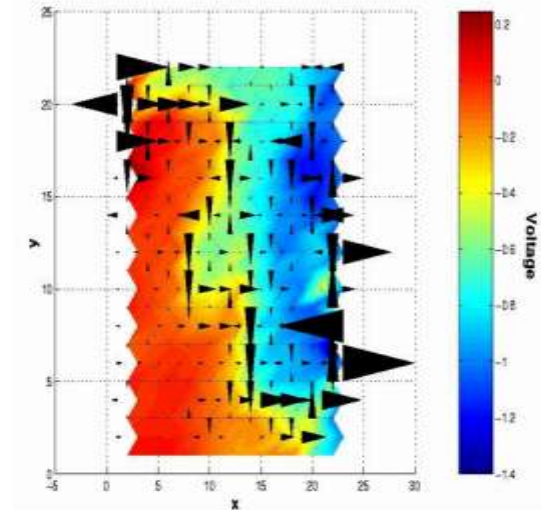
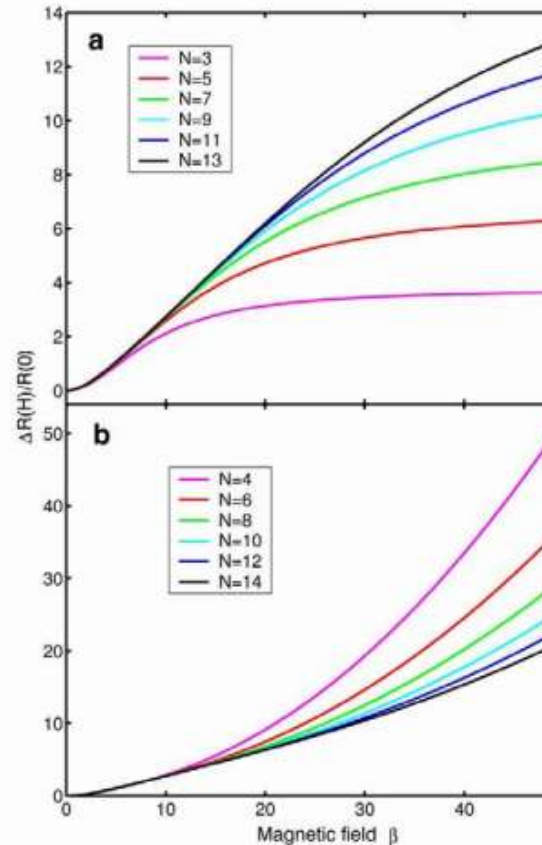
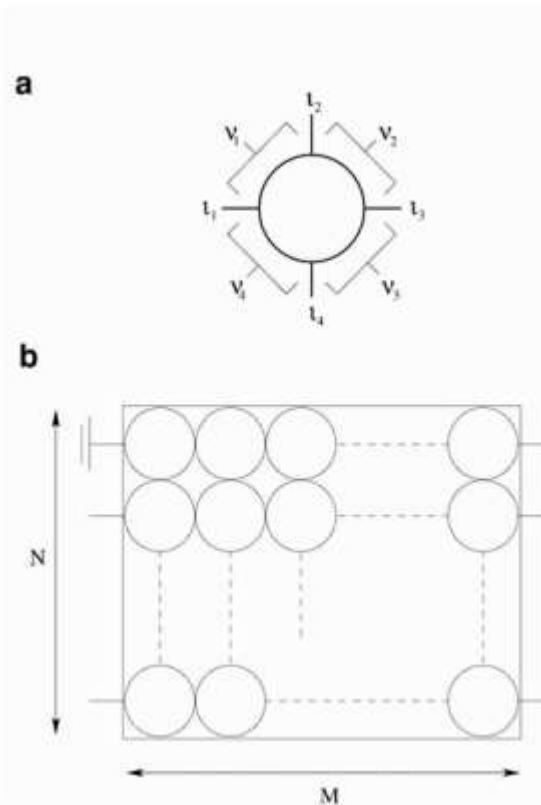


Figure 3 Visualisation of currents and voltages at large magnetic field in a 10×10 random network of disks with radii 1 (arbitrary units), where the potential difference $U = -1V$. The black arrows represent the currents, where arrow size depicts the magnitude of the current. The major current path is perpendicular to the applied voltage a significant proportion of the time, which implies that the magnetoresistance is provided internally by the Hall effect, which is therefore linear in H .

$$R_{NM} = \frac{U}{\sum_i I_i} = \frac{U}{\sum_i Z_{ij}^{-1} V_j}$$

where $\beta = \mu H$, μ is the carrier mobility

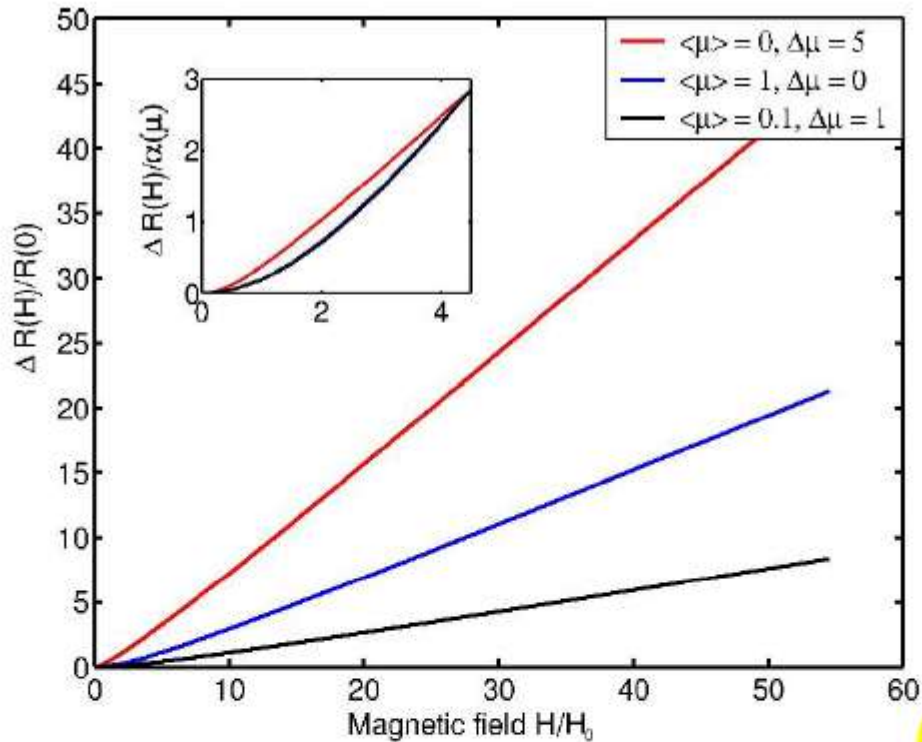


Figure 4 Average normalised magnetoresistance $\Delta R(H)/R(0)$ as a function of dimensionless magnetic field H/H_0 of 20×20 random resistor networks for different mobility distributions, where $H_0 = 1\text{kOe}$ is a typical field scale. The magnetoresistance was averaged over 10 random network configurations and the mobility distributions were taken to be Gaussian and measured in units of

Magnetocapacitance in non-magnetic inhomogeneous media

Meera M. Parish PRL, 101, 166028 (2008)

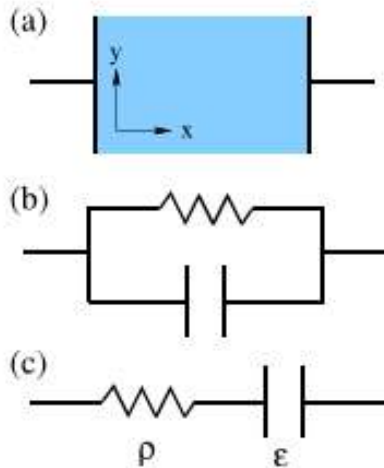


FIG. 1: Simple circuits of resistors $\hat{\rho} \equiv \hat{\sigma}^{-1}$ and capacitors ϵ that illustrate the basics of dielectric response. Diagram (a) depicts the measuring set-up, where a rectangular sample is confined between metallic plates and subjected to an applied electric field $E_x \hat{x}$, (b) represents a simple homogeneous medium, and (c) represents the simplest metal-insulator composite that exhibits the Maxwell-Wagner effect.

$$\Re[\epsilon_{xx}(\omega)] = \frac{\epsilon(1 - \beta^2 + (\omega\tau)^2(1 + \beta^2)^2)}{1 + (\omega\tau)^2(1 + \beta^2)^2}$$

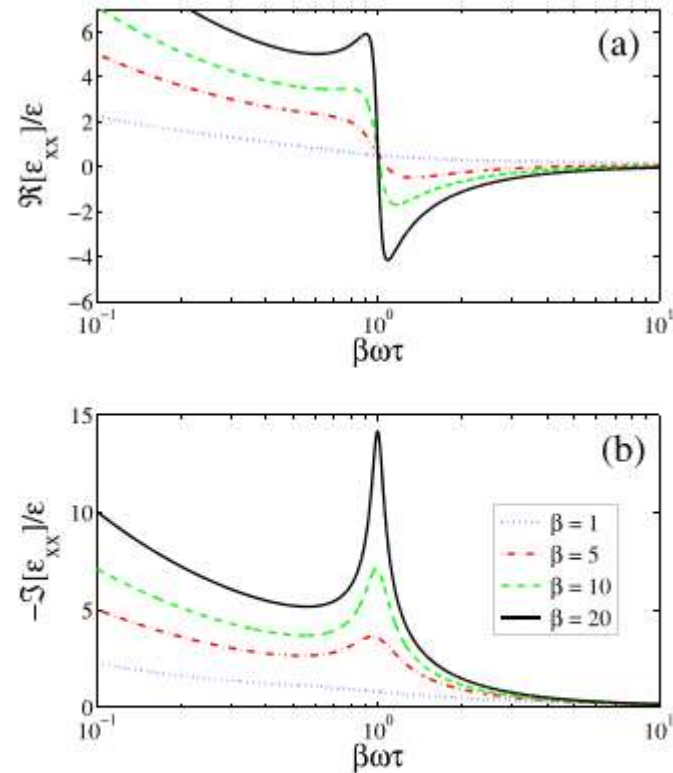
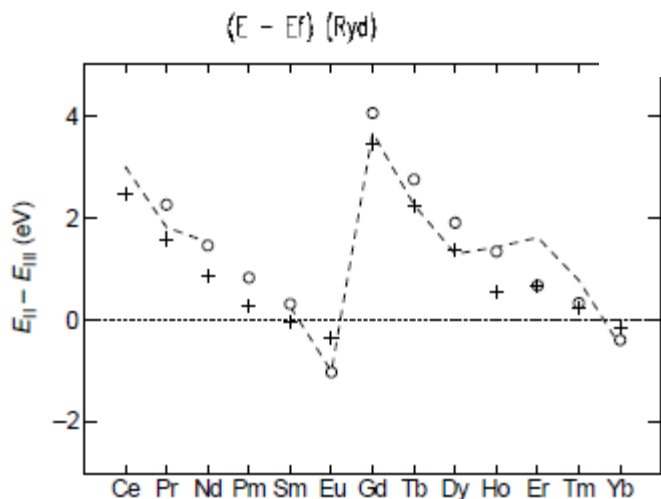
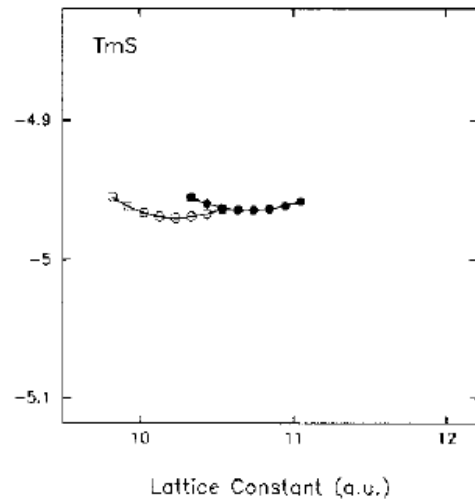
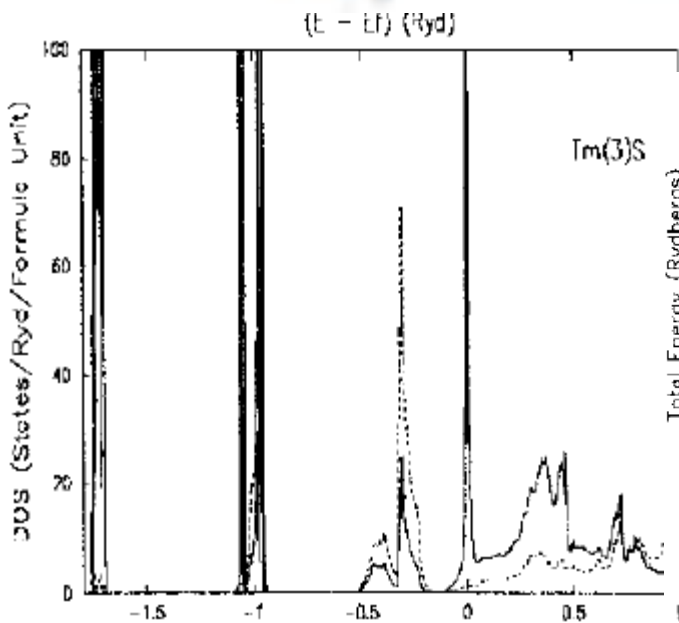
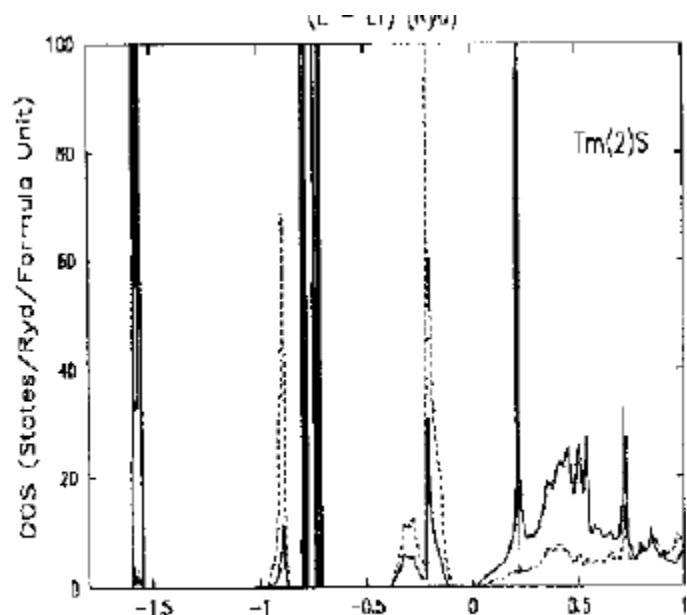
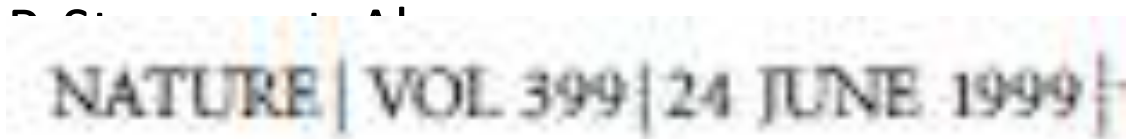
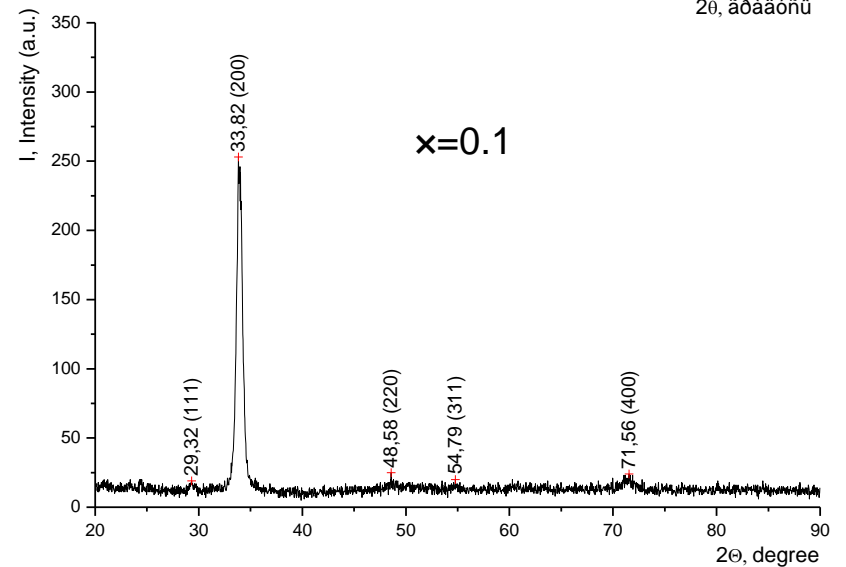
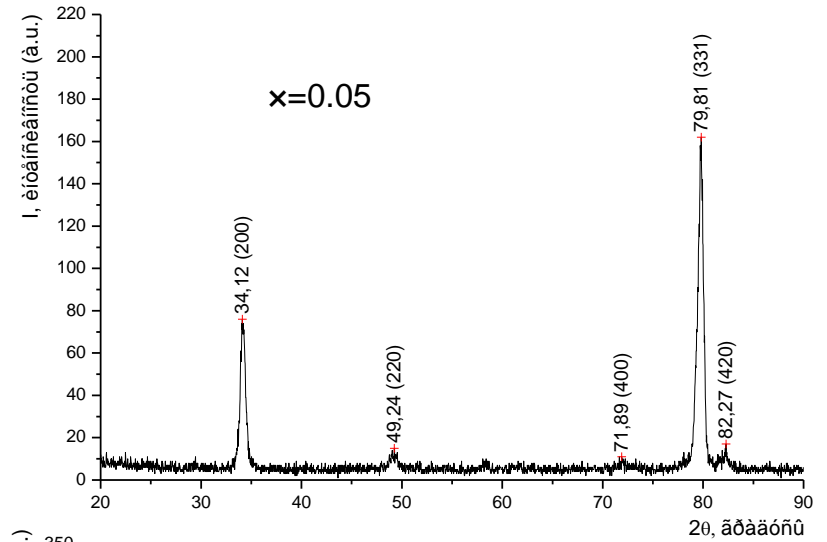
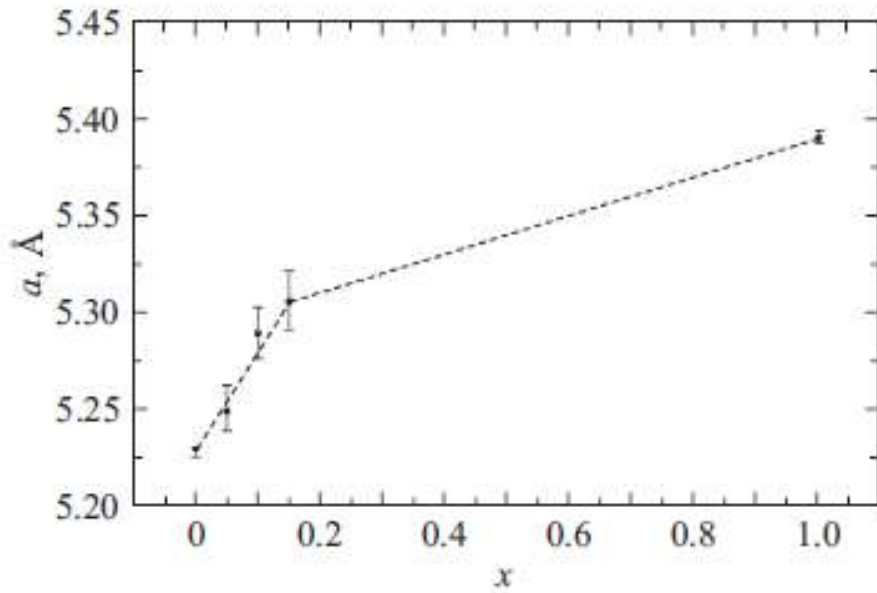


FIG. 2: Dielectric response versus frequency over a range of magnetic fields β for a 2D two-component medium with equal proportions ($p = 1/2$). When $\beta > 1$, there is a resonance at normalized frequency $\beta\omega\tau = 1$, where the real part (a) varies rapidly, eventually changing sign, while the imaginary part (b) exhibits a peak.

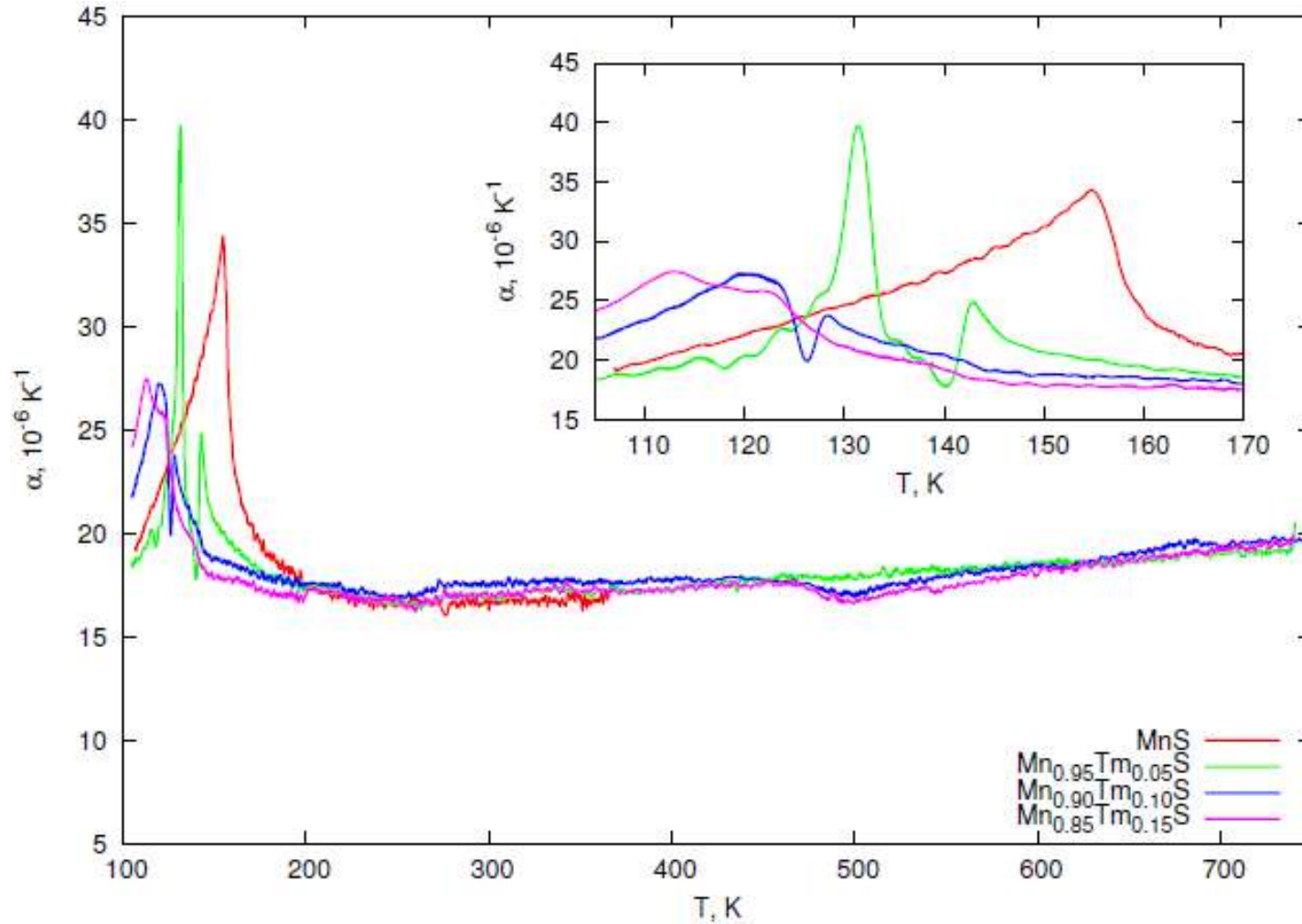
Electron structure of divalent and trivalent thulium in TmS



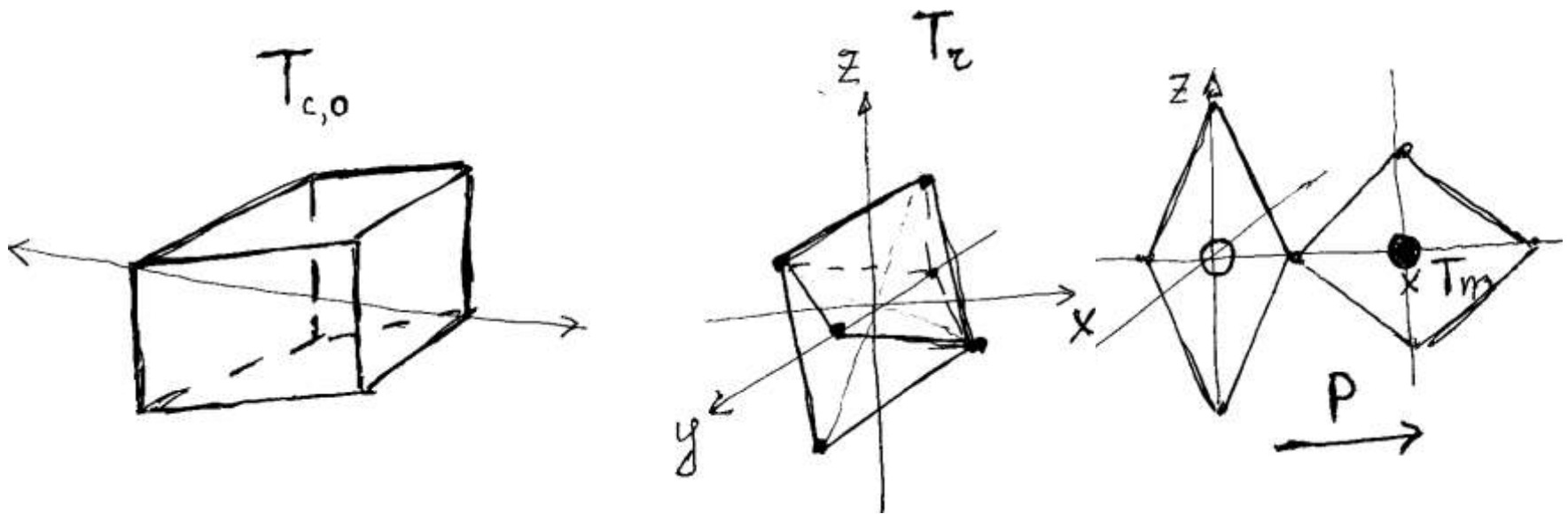
X-ray and lattice constant $Tm_xMn_{1-x}S$



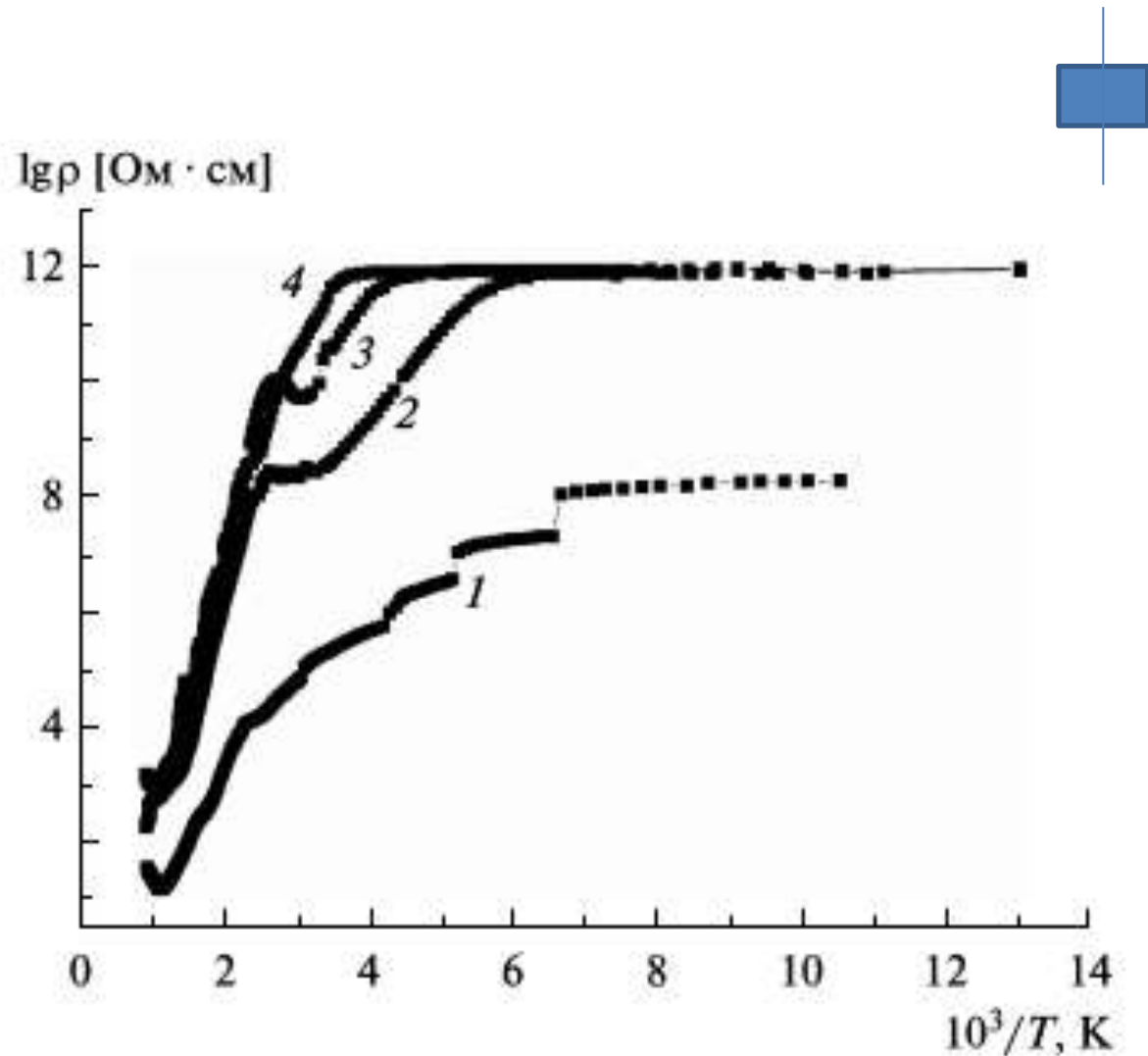
Thermal expansion coefficient $Tm_xMn_{1-x}S$ for $x=0, 0.05, 0.1, 0.15$.



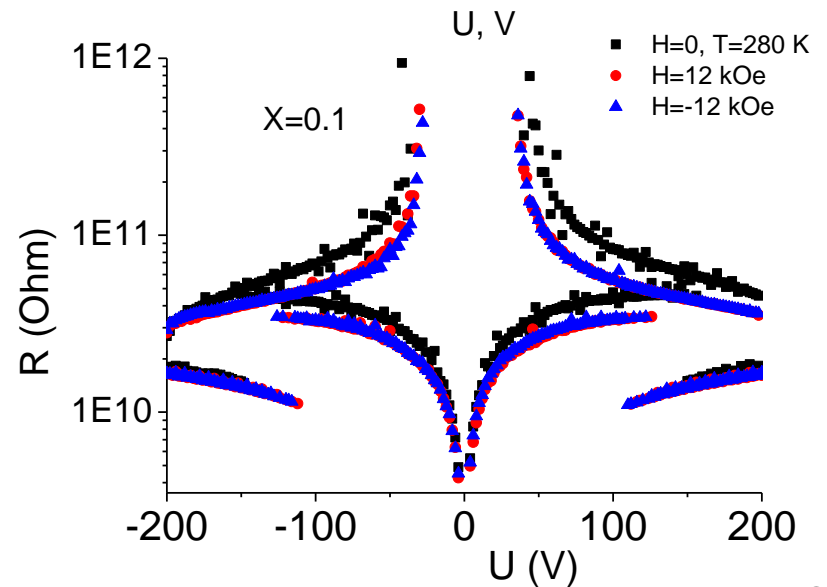
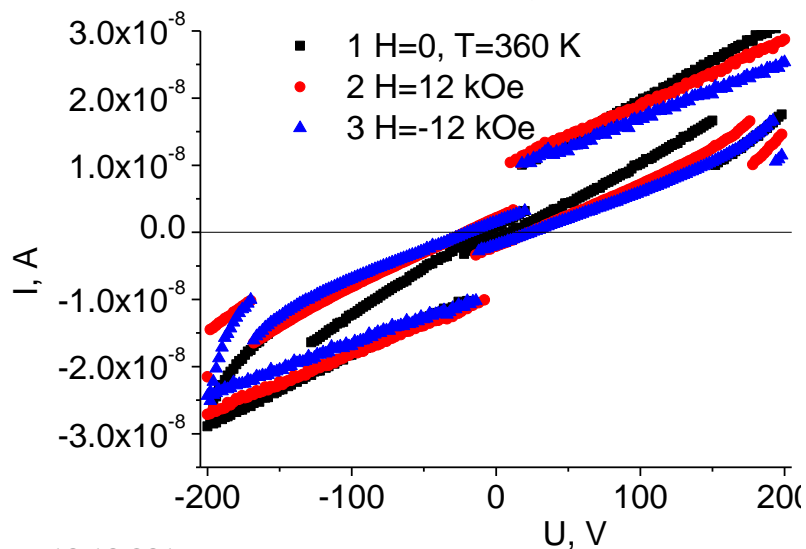
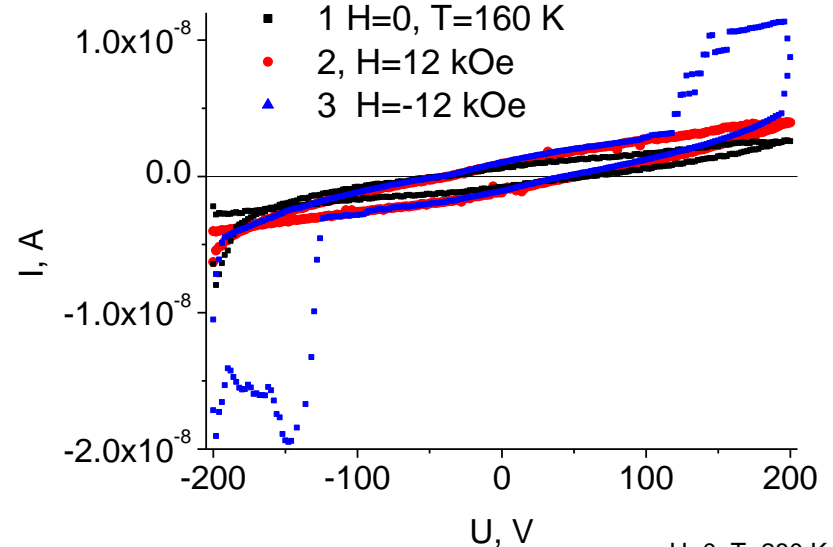
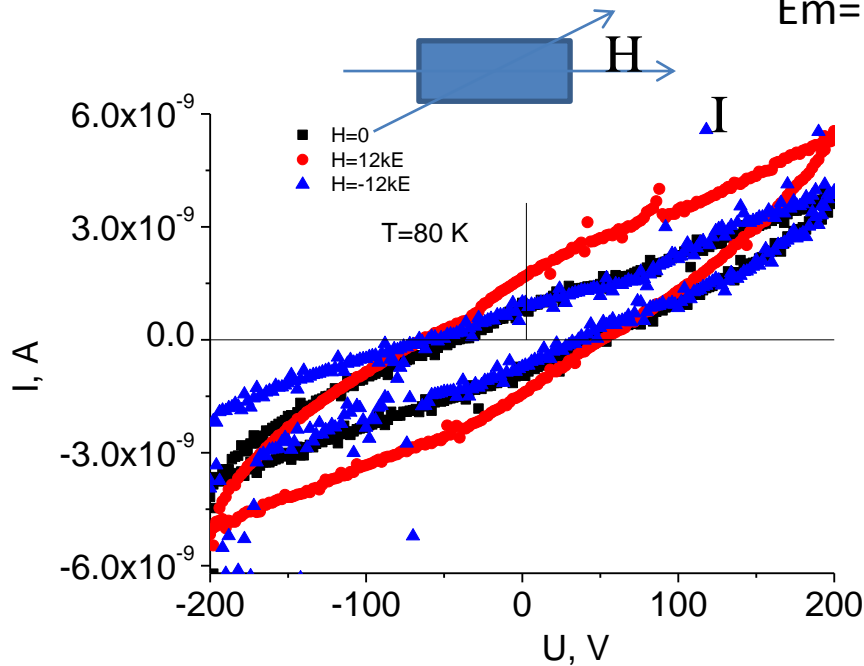
Deformation of crystal structure versus temperature



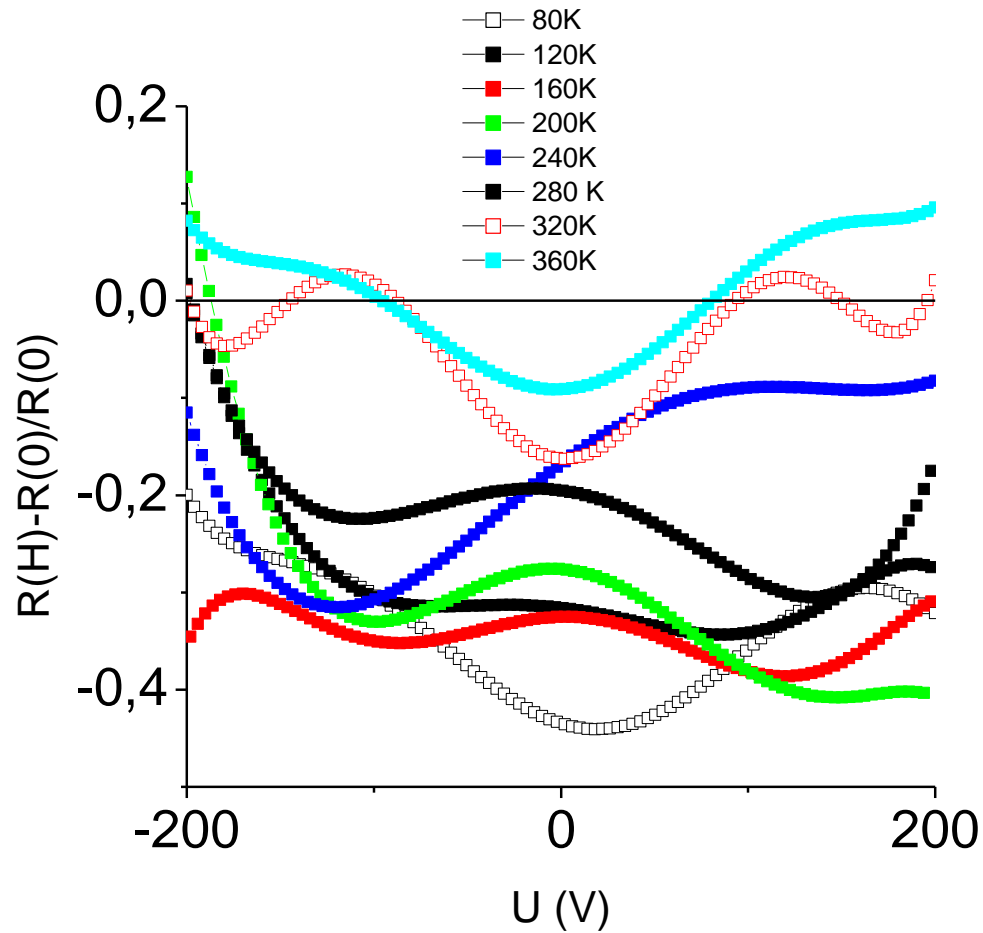
Resistance of $Tm_xMn_{1-x}S$ $x=0.05$ (2), 0.1 (3), 0.15 (4) measured by two contact method (b) .



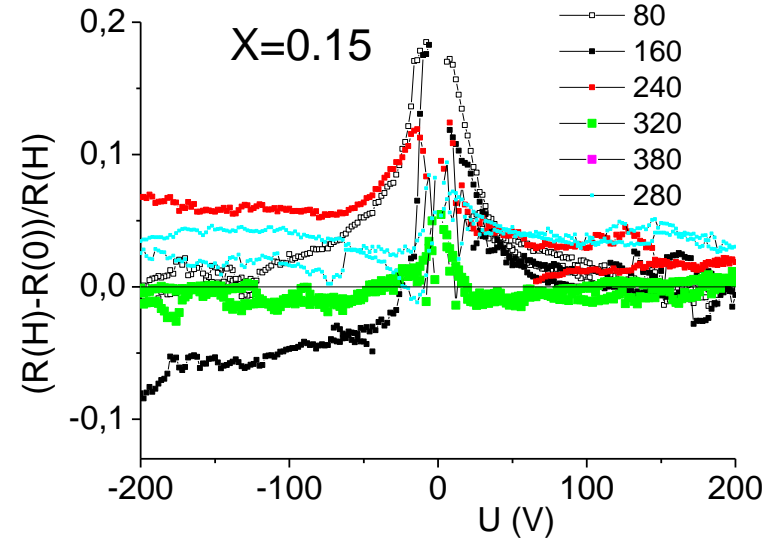
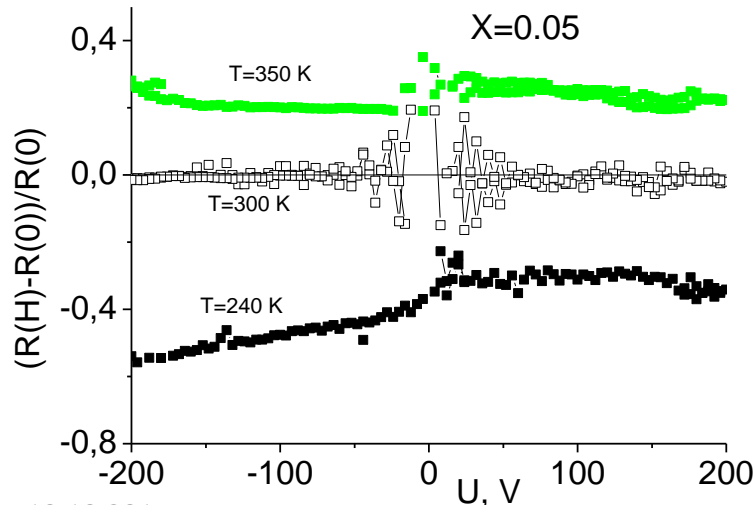
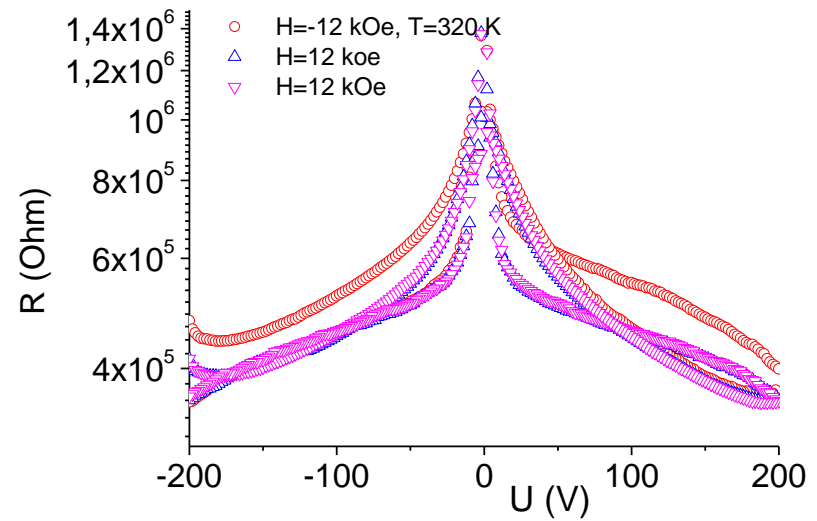
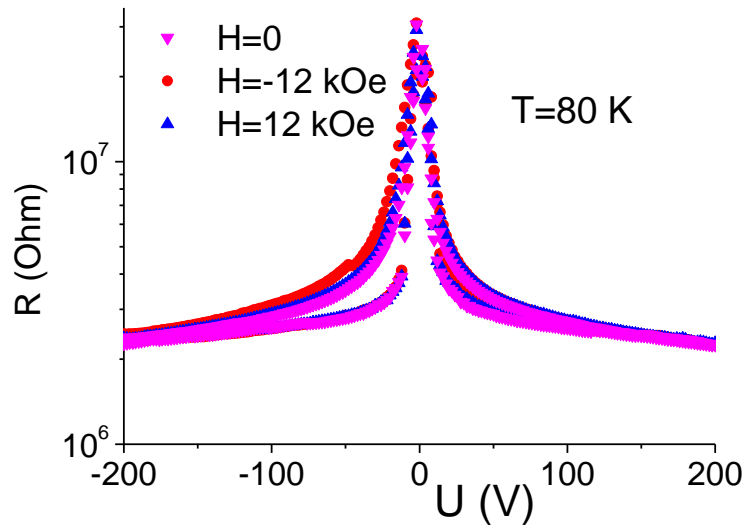
TmxMn1-xS with $x = 0.1$ current voltage characteristic at temperatures $T = 80$ K, 160 K, 360 K in magnetic fields $H = 0, 12$ kOe, -12 kOe. Electric field maximum is $E_m = 1000$ V/cm



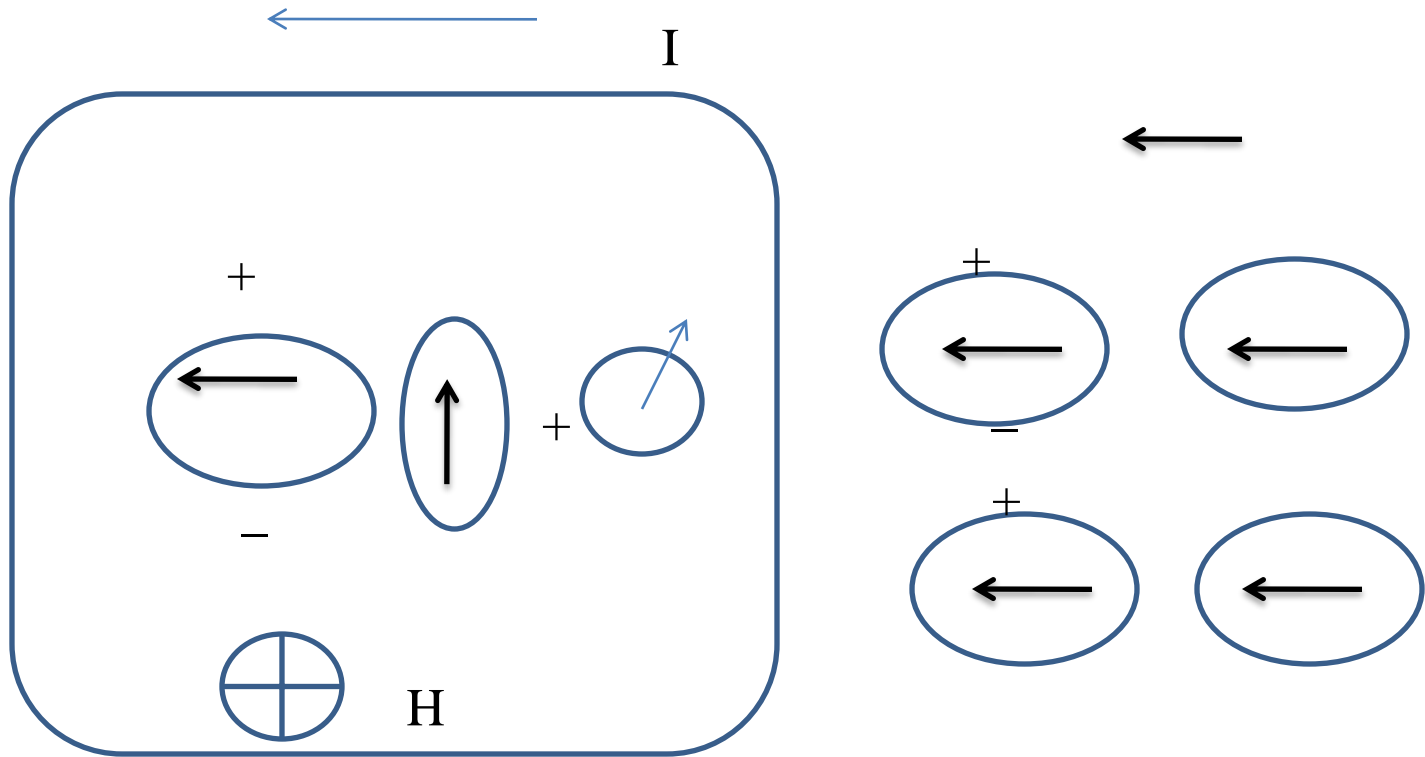
Magnetoresistance $Tm_xMn_{1-x}S$ with $x = 0.1$ determined by current voltage characteristic at $H=12$ kOe

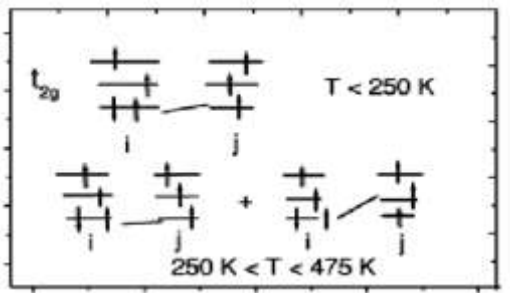
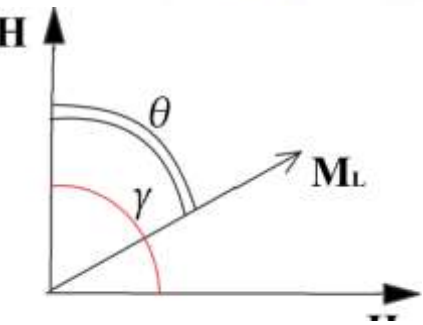
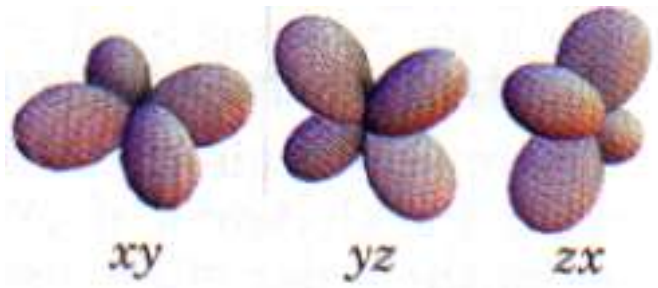


Resistance and Magnetoresistance $Tm_xMn_{1-x}S$ with $x = 0.05, 0.15$ determined by current voltage characteristic at $H=12$ kOe



Charging region



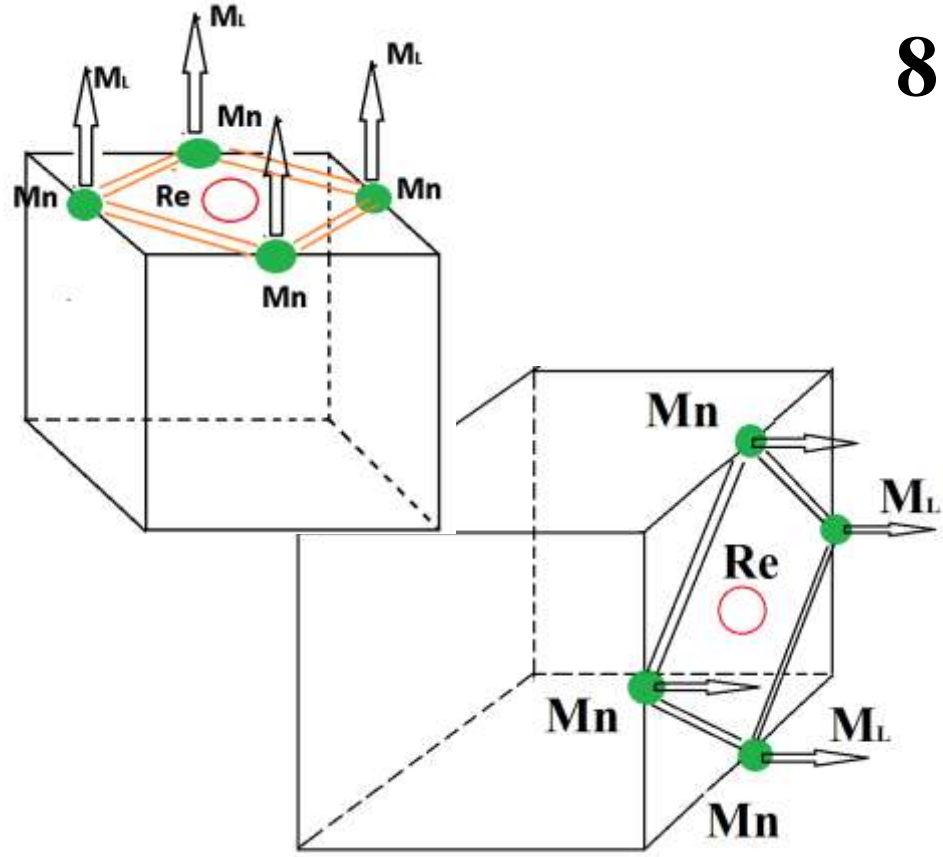


$$\frac{\rho(H) - \rho(0)}{\rho(0)} = \frac{1}{1 + xP_1P_2\cos\theta} - 1,$$

$$W = M_L H \cos\theta + M_L H_A \cos(\gamma - \theta)$$

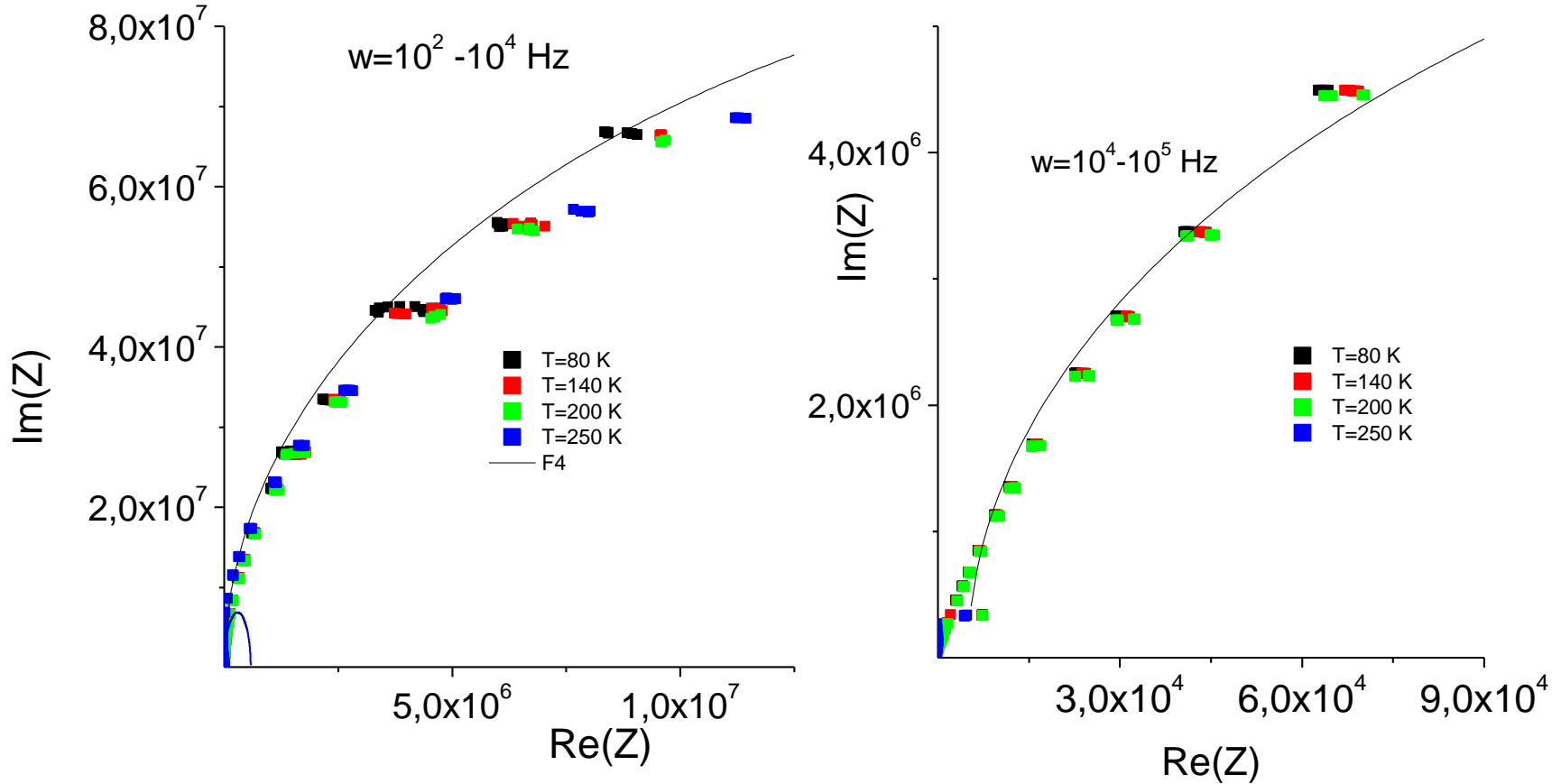
$$\cos\theta = 1 / \sqrt{\left(1 + H_A^2 \sin^2 \gamma / (H + H_A \cos \gamma)^2\right)}.$$

$$\text{tg } \theta = H_A \sin \gamma / (H + H_A \cos \gamma).$$

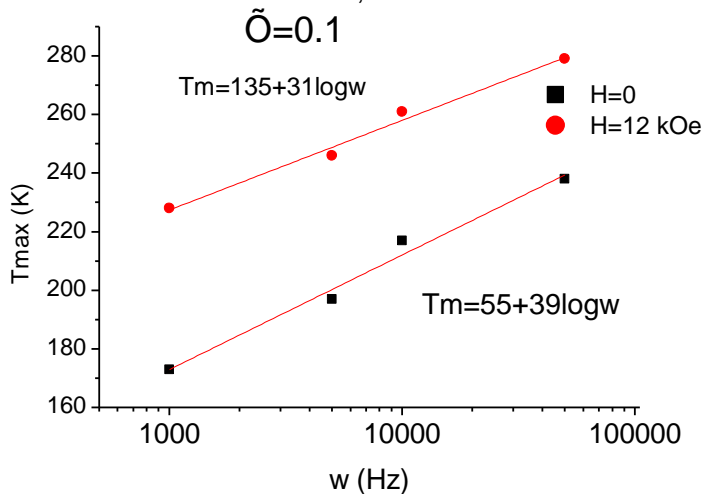
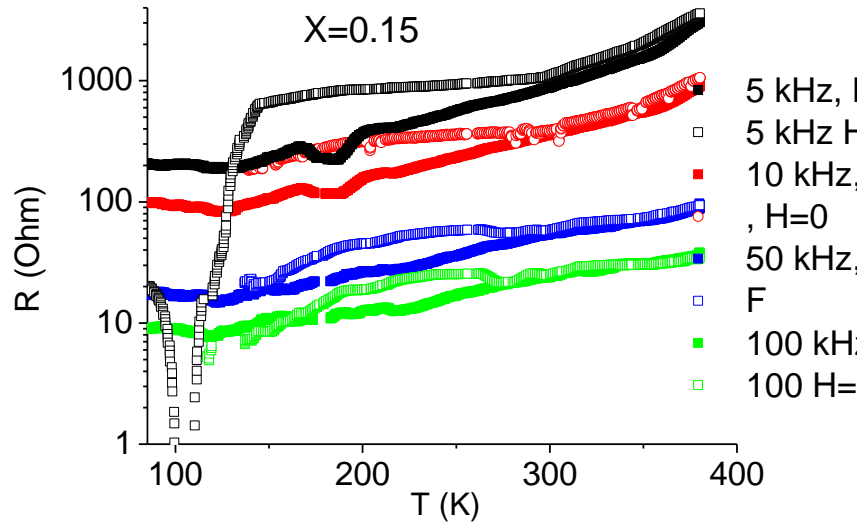
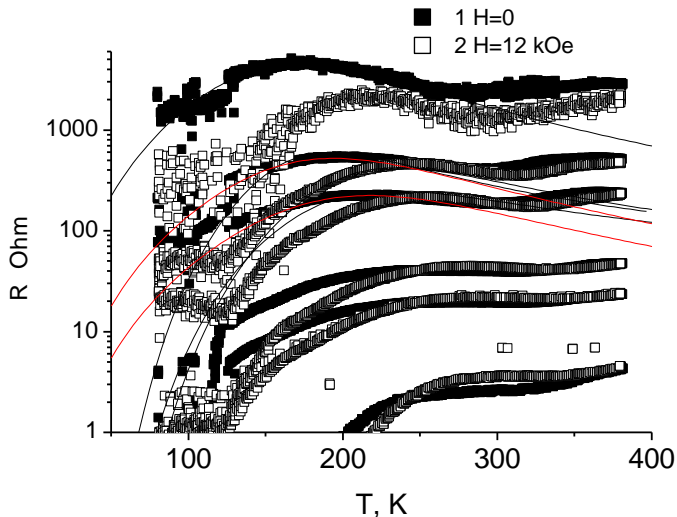


γ - угол между осью анизотропии и внешним магнитным полем где $\lambda = H/K$, K - константа анизотропии

Годограф импеданса Tm01Mn09S

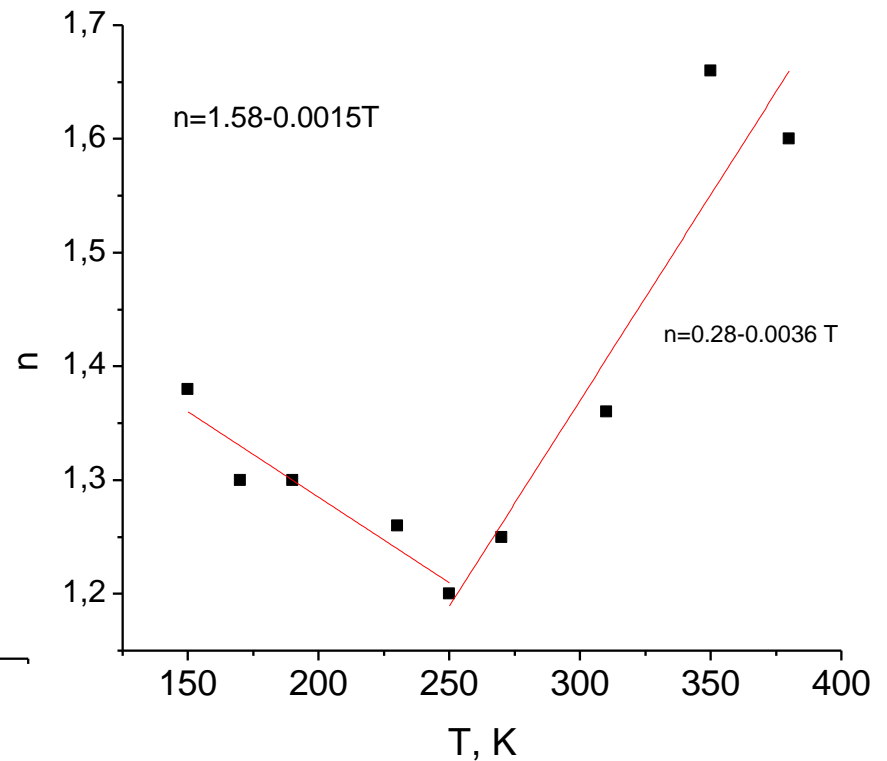
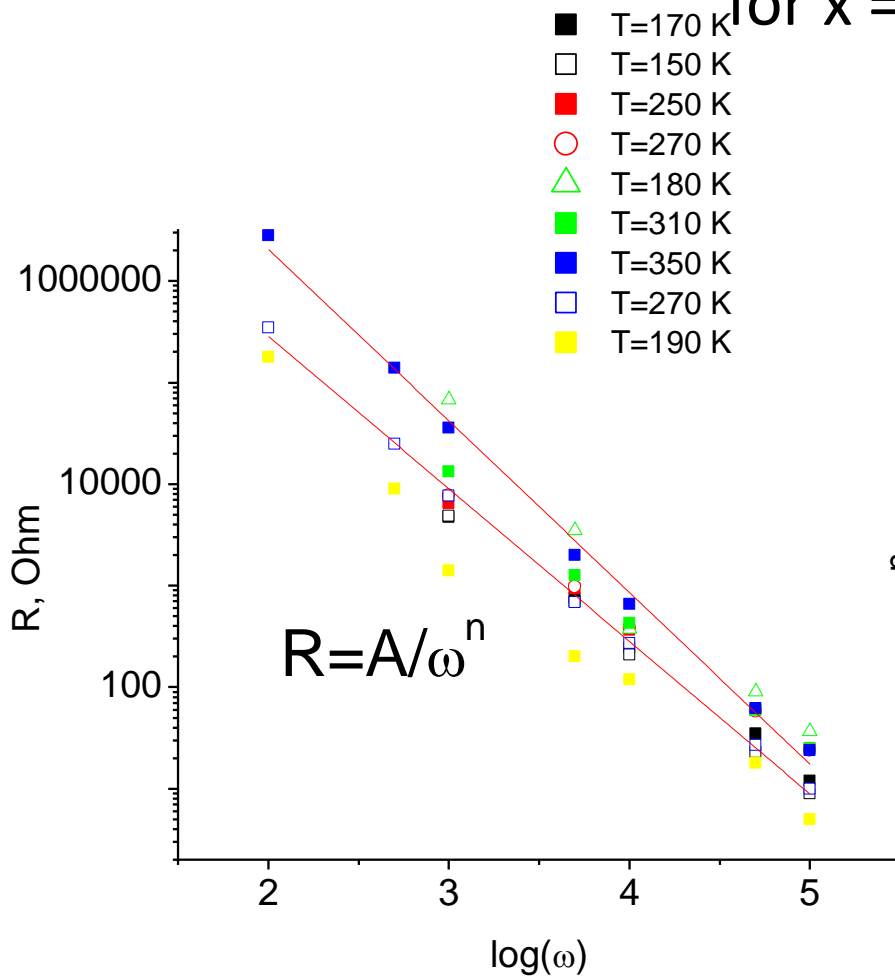


The active resistance in a zero magnetic field and in the field $H=12 \text{ k}\mathcal{A}$ from temperature at frequencies $\omega=1 \text{ kHz}, 5 \text{ kHz}, 10 \text{ kHz}, 50, 100, 300 \text{ kHz}$.

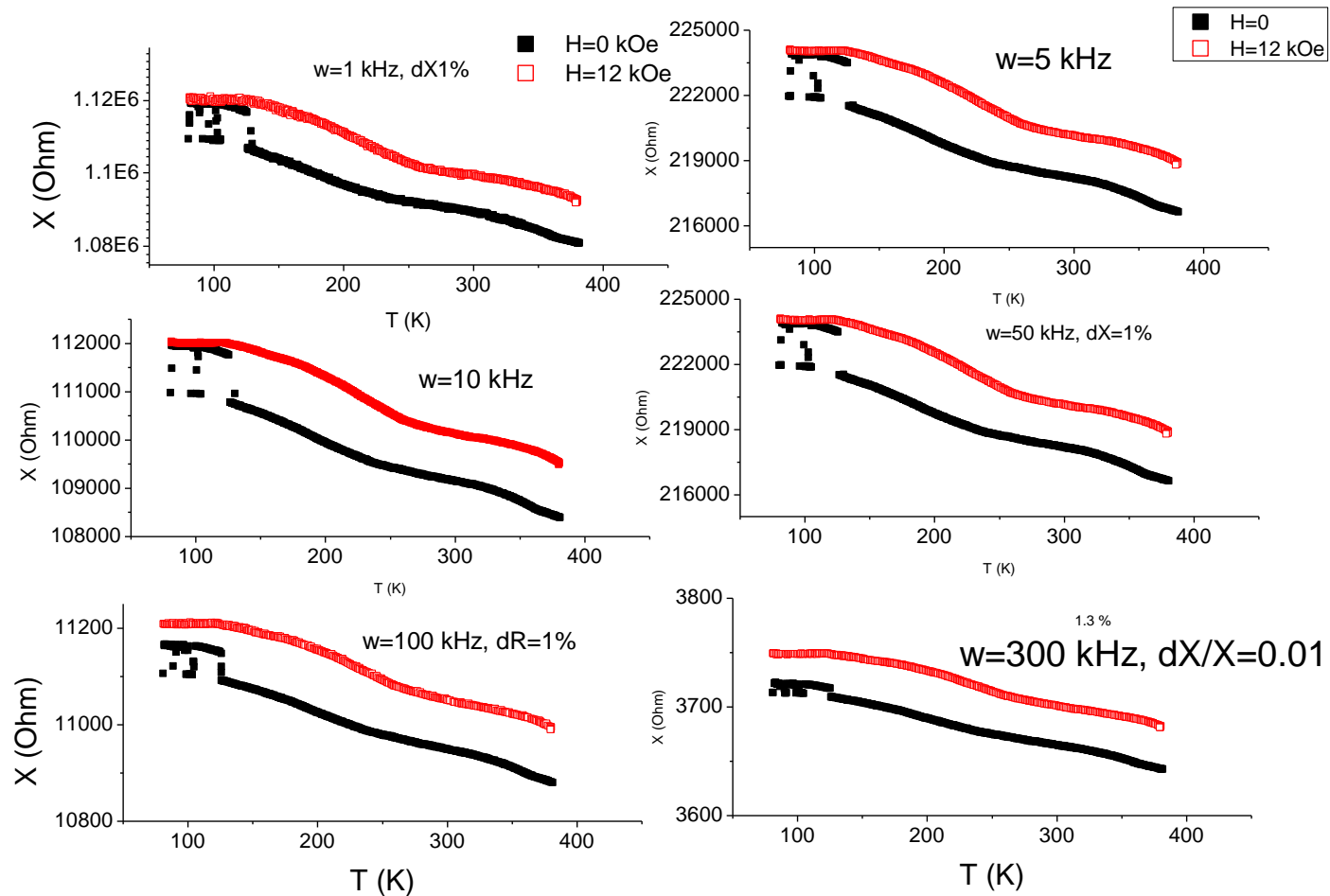


$$R = \frac{\text{Im}(\chi)}{\omega} = \frac{\tau}{1 + (\omega\tau)^2} \quad \tau = (530 - 100 \log \omega) / (\omega^{1/3} T^2)$$

Resistance from frequency at the fixed temperature for $x = 0.15$

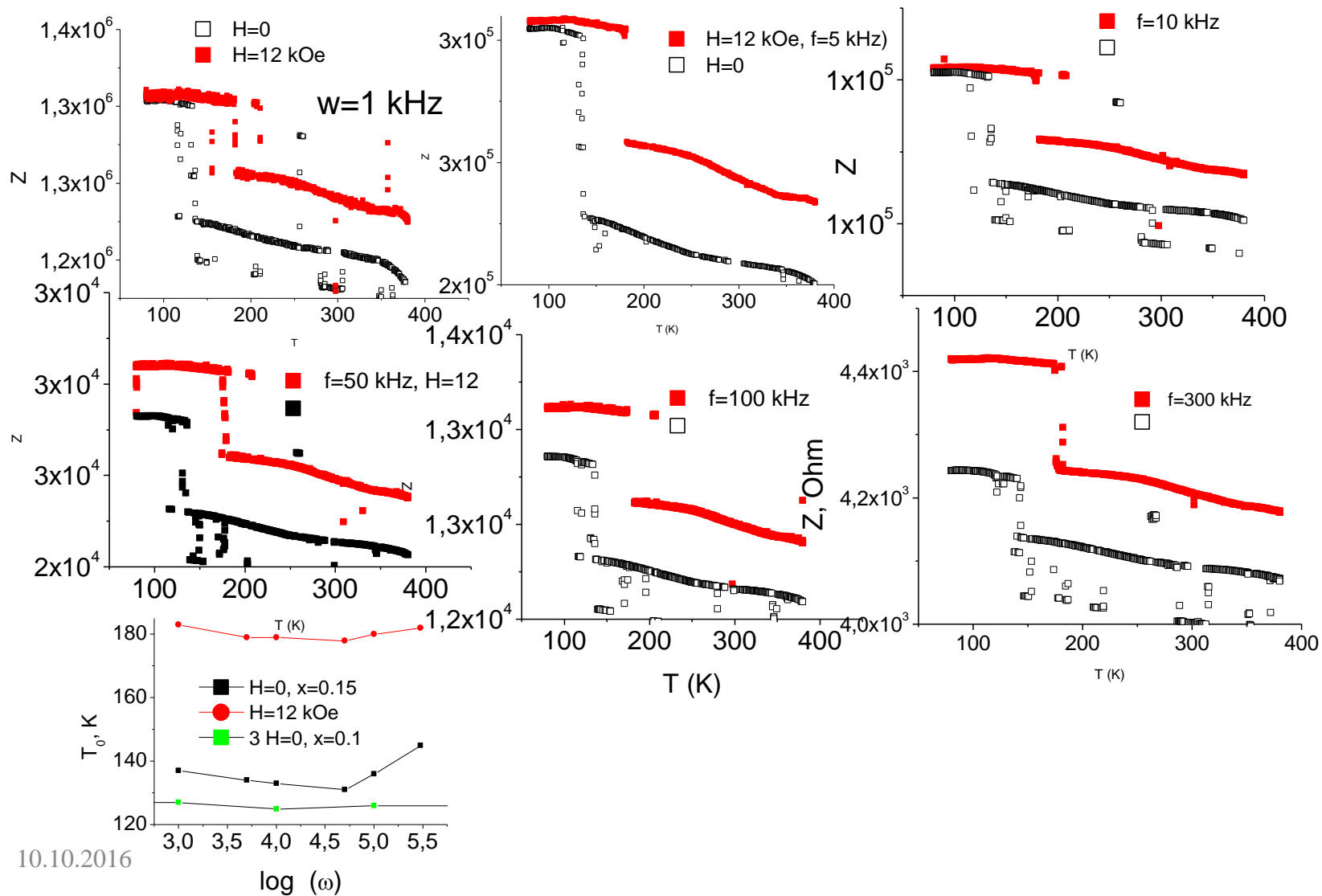


Imaginary resistance from temperature in $Tm_xMn_{1-x}S$ for $x = 0.1$ on frequencies $w=1, 5, 10, 50, 100$ и 3000 kHz

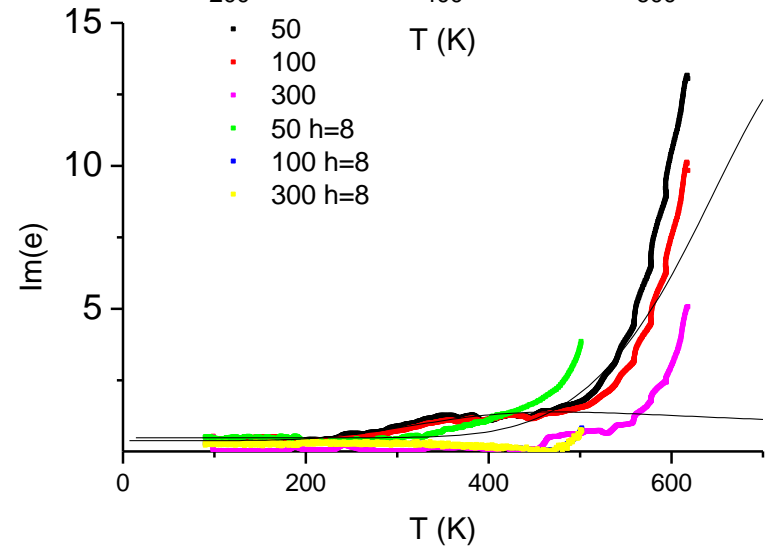
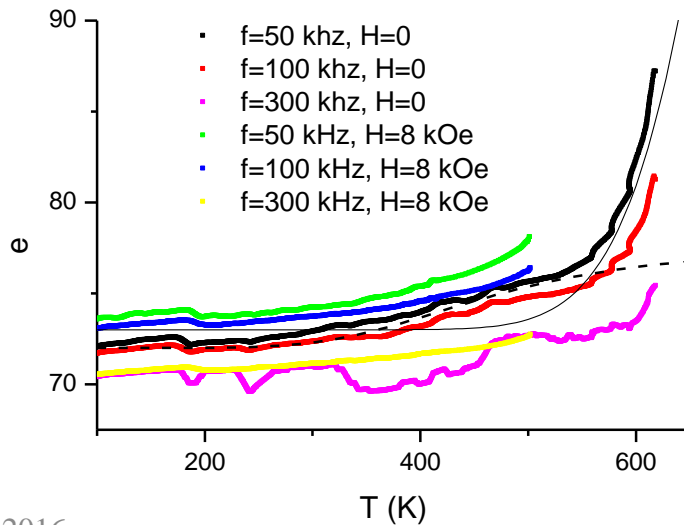
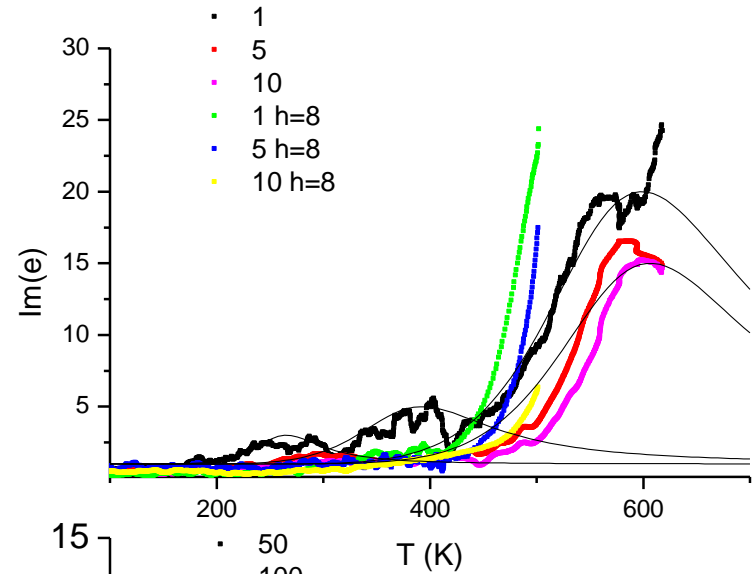
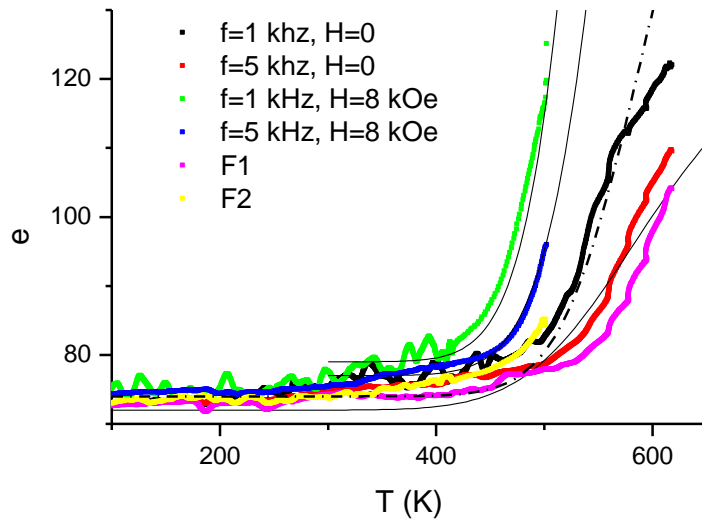


$$L_{\text{induct}} \sim \langle S_i S_j \rangle \langle L_i L_j \rangle$$

Impedance from temperature in $Tm_xMn_{1-x}S$ for $x = 0.15$ at frequencies $w=1, 5, 10, 50, 100$ и 3000 kHz



Real and imaginary permittivity from temperature without field and in a magnetic field for X = 0.1

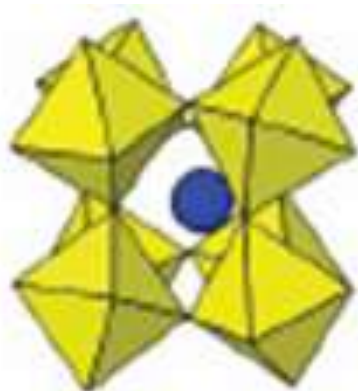


Диэлектрическая восприимчивость в модели Дебая

12

$$\text{Re}(\chi)/N = \chi_{L0} + \chi_0 / (1 + (\omega\tau_g)^2) + \chi_0 / (1 + (\omega\tau_c)^2)$$

$$\text{Im}(\chi)/N = \chi_0 \omega \tau_g / (1 + (\omega\tau_g)^2) + \chi_0 \omega \tau_c / (1 + (\omega\tau_c)^2)$$

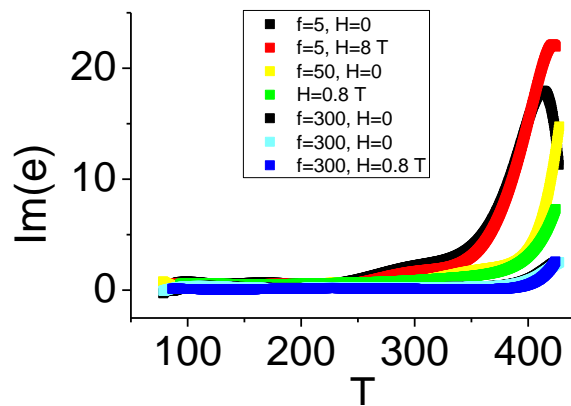
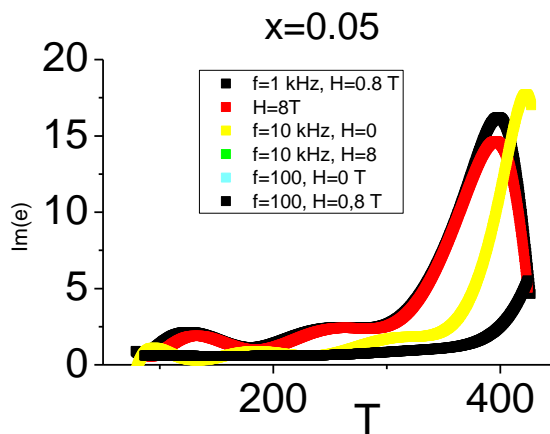


Время релаксации диполей:

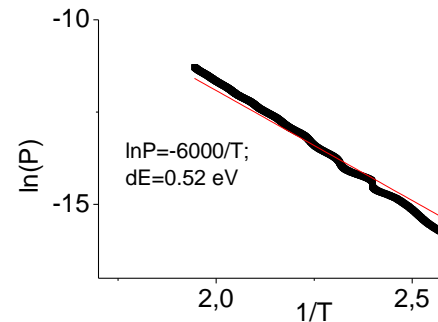
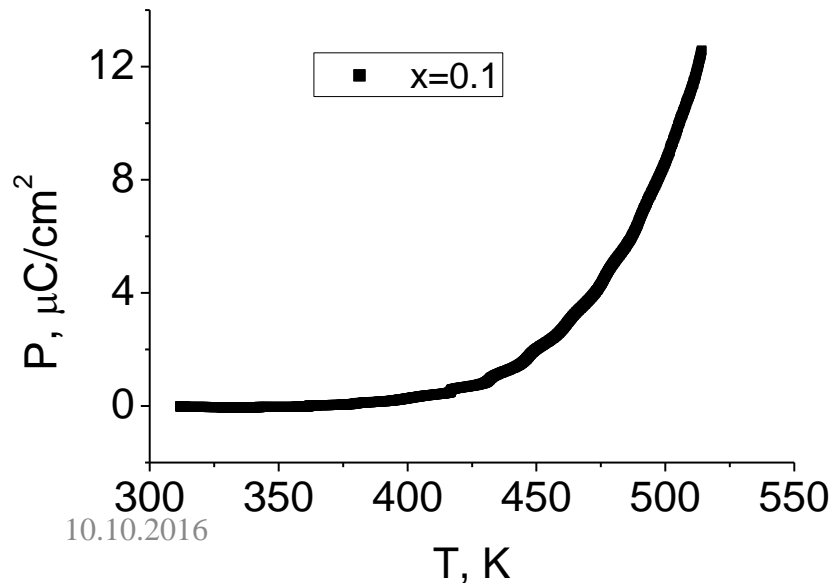
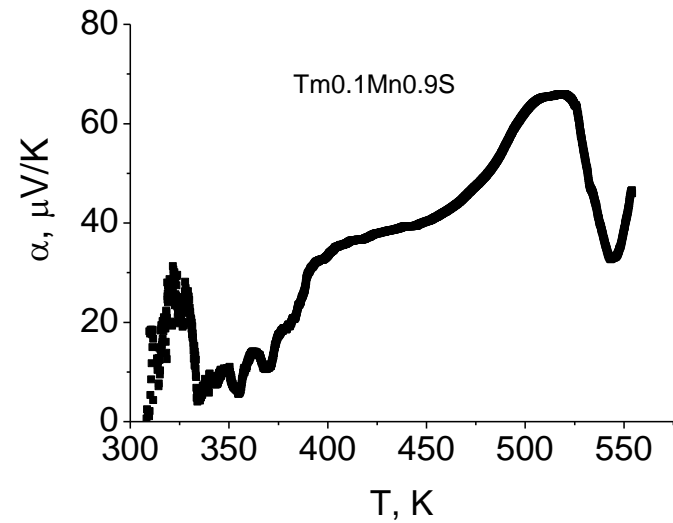
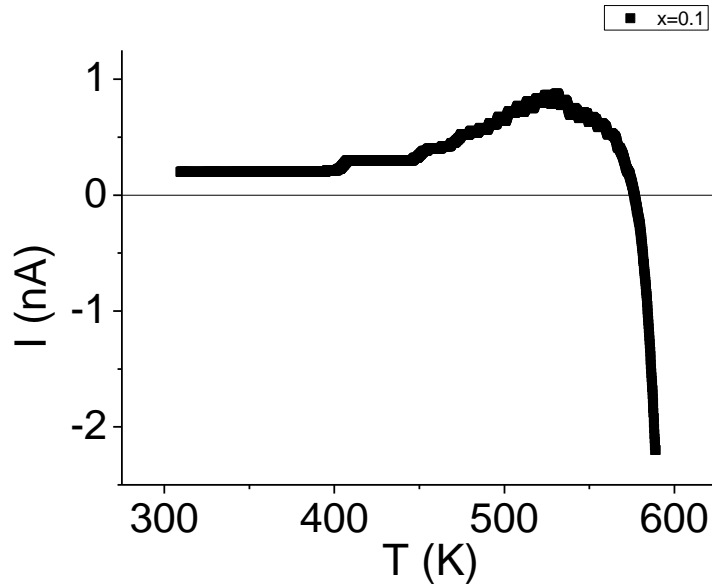
$\tau_g = \tau_0 \exp(\Delta E/kT)$, где ΔE – энергия активации.

$$\Delta E_1 = 0.18-0.2 \text{ eV};$$

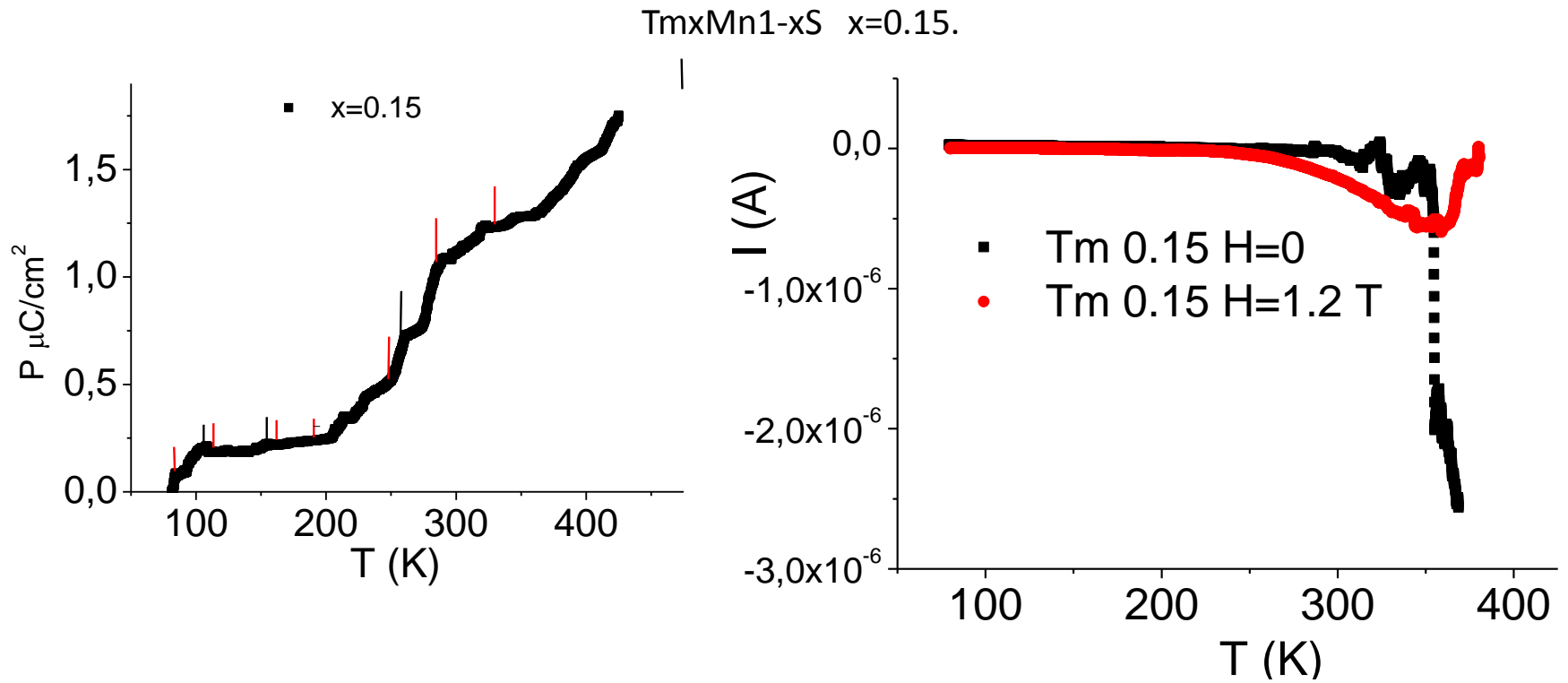
$$\Delta E_2 = 0.36 \text{ eV}, x=0.1$$



Pyrocurrent, polarization, thermoeds of $Tm_{0.1}Mn_{0.9}S$



Polarization, pyrocurrent and thermal expansion coefficient for



Pyrocurrent, polarization of $Tm_xMn_{1-x}S$ versus temperature for $x=0,05$

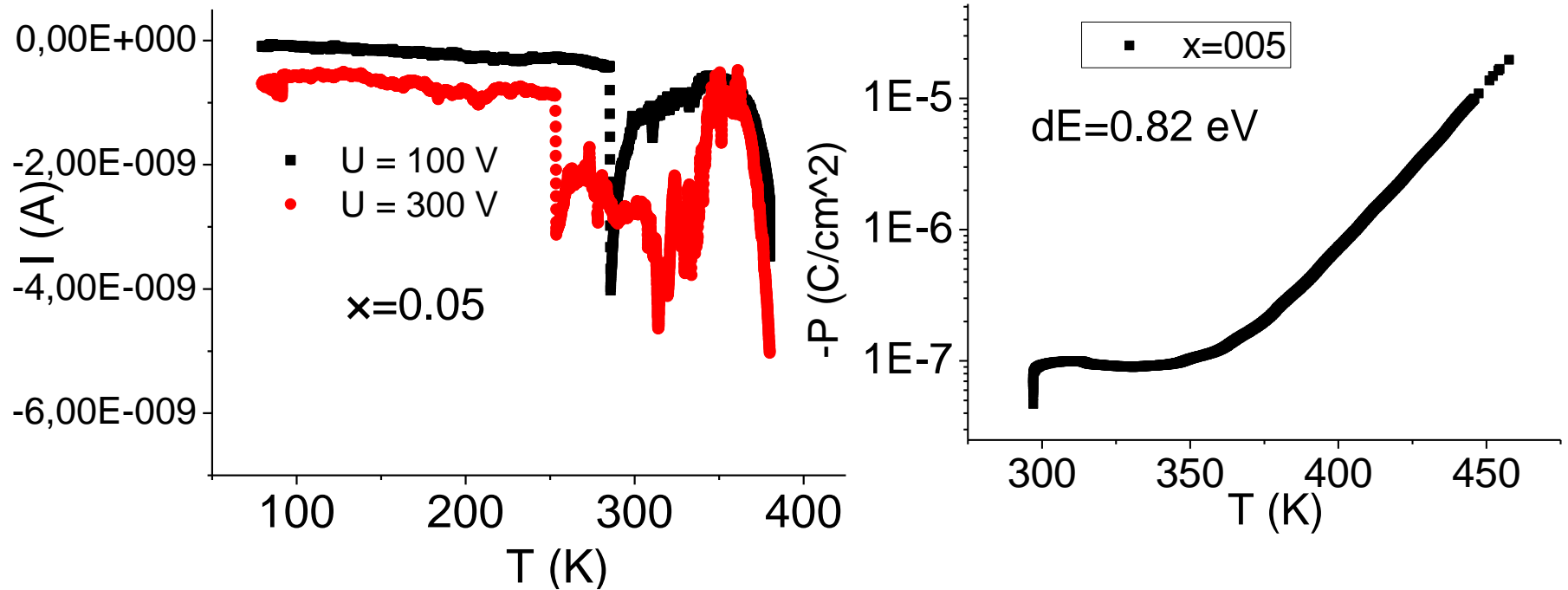
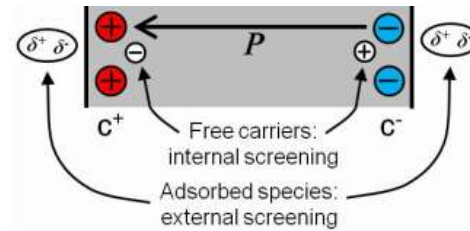
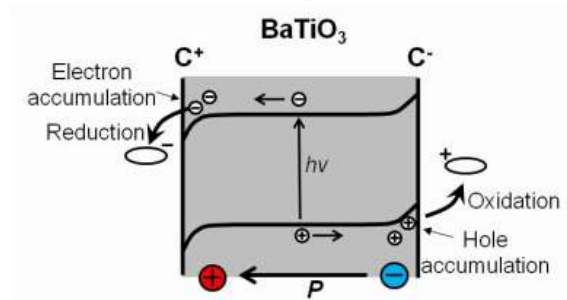


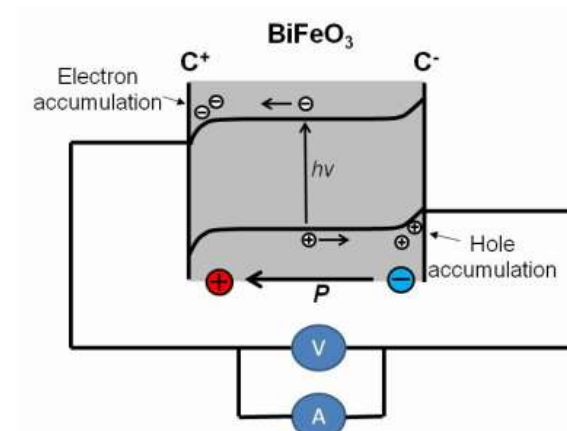
Figure 12: Influence of ferroelectricity on carrier movement arising from (a) internal polarisation and screening mechanisms and (b) effect of free carrier reorganisation on band structure and photoexcited carriers. And (c), the influence on band bending in a ferroelectric material on carriers to generate a photovoltaic system.



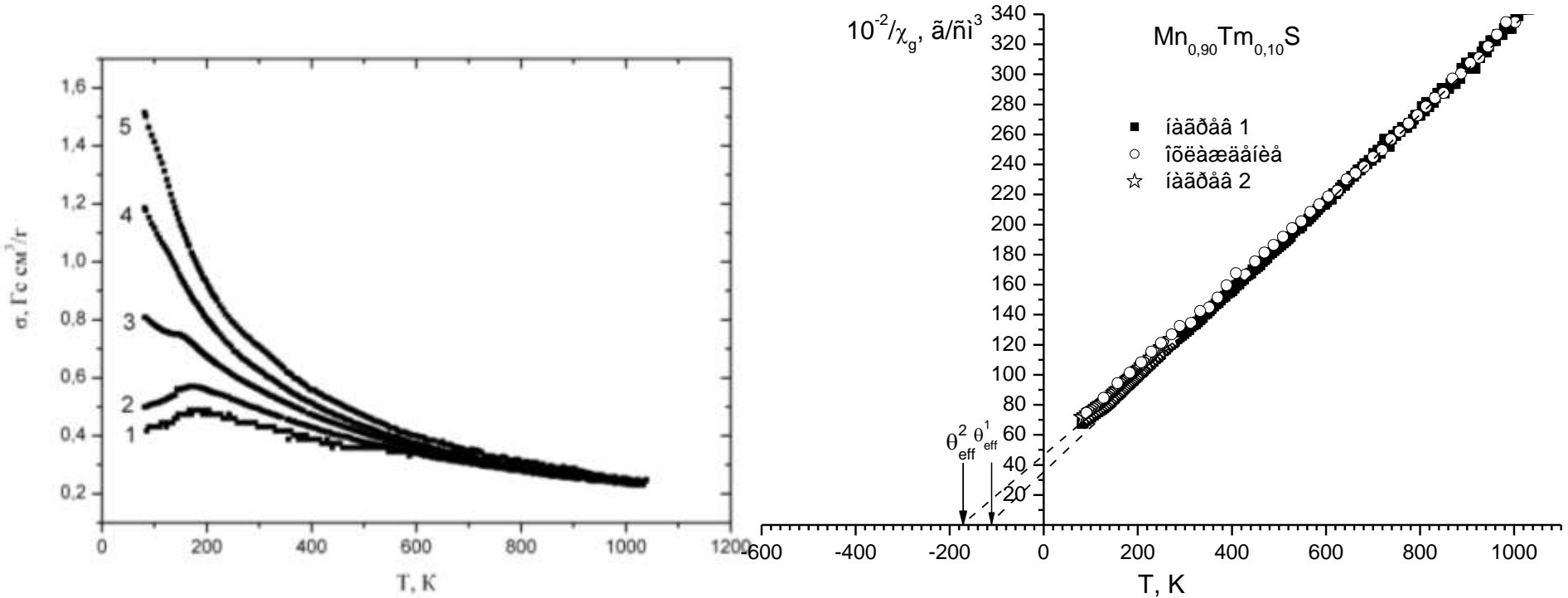
(a)



(b)



Magnetic moment in $Tm_xMn_{1-x}S$ for $x = 0, 0.05, 0.1, 0.15$ in the field of $H=8.6$ kOe and the inverse susceptibility for $x = 0.1$ from temperature

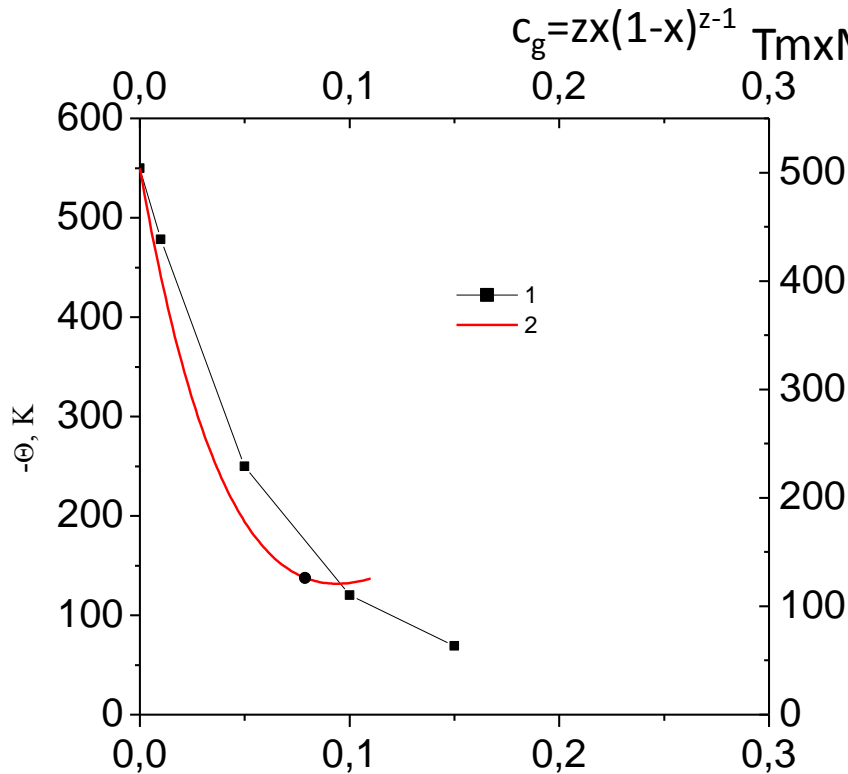


$$H = -\sum J_{ij} S_i S_j - \sum J_{so} (L_i L_j) (S_i S_j) - \sum J_0 (L_i L_j)$$

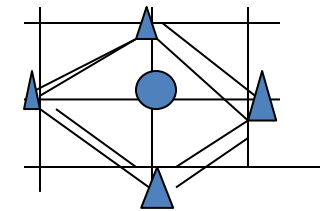
$$\chi_s(Q) = \frac{T + J_m(Q)/4(1 - M_L^2)}{T^2 + \frac{T}{4}[J_m(Q) - J_s(Q)] - 9/4 J_m J_s (1 - M_L^2)}$$

Э.Л. Нагаев, Наука, М. (1988), 231с

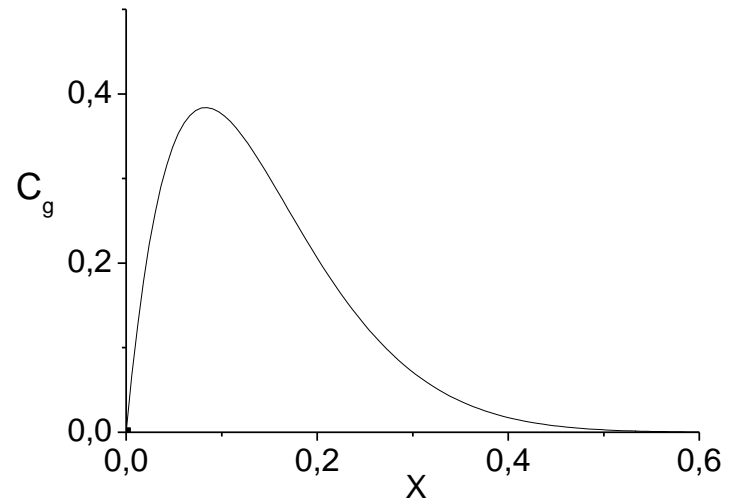
Paramagnetic Curie temperature: experiment (1) and calculation in a molecular field (2) $\Theta(x) = \Theta_{MnS} (1-x-\lambda cx)$ with fitting parameter $\lambda = J^*(Mn-Mn) / J(Mn-Mn) = 1.75$,



$$c_g = z x (1 - x)^{z-1}$$



μ_{eff}^{Mn}



Магнитный момент на один ион от температуры

$$\mu_{eff} = (3kC/N_{\mu B}^2)^{1/2} = 6-5.2$$

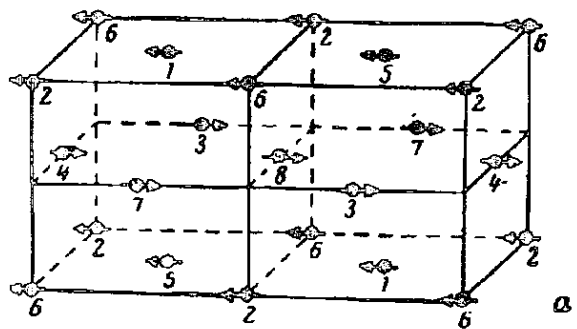
Conclusion

- Sharp falling of paramagnetic Curie temperature in the range of concentration $0 < x < 0.1$ in solid solutions $Tm_xMn_{1-x}S$ is found in results of formation ferromagnetic exchange in the vicinity of thulium ions.
- For all compounds the magnetoresistance in $Tm_xMn_{1-x}S$ at temperatures several times exceeding Neel temperature is found .
- Magnetic characteristics and magnetoresistance is explained in terms of orbital-charging model.



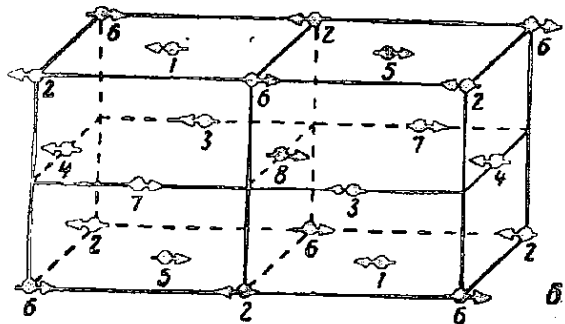
Thank you for your attention

Антиферромагнитное упорядочение первого (а), второго (б), и третьего (в) родов в ГЦК решетке



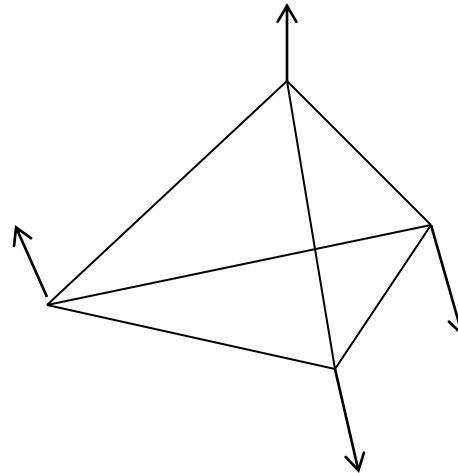
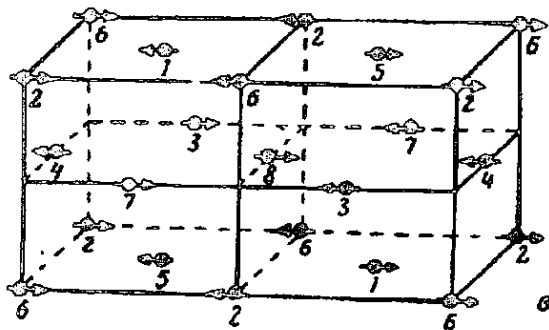
$T_N = 2/3 S(S+1) z_2 J_2$, где J_2 - обмен во 2-ой координационной сфере, $z_2=6$

$$\Theta_P = 2/3 S(S+1) (z_1 J_1 + z_2 J_2), z_1=12$$



$$\theta(x) = \theta_{MnS} (1 - x - \lambda_{MnMn} c_g - \lambda_{MnRe} x),$$

$$\lambda_{MnRe} = I_{MnRe} / K_{MnMn},$$

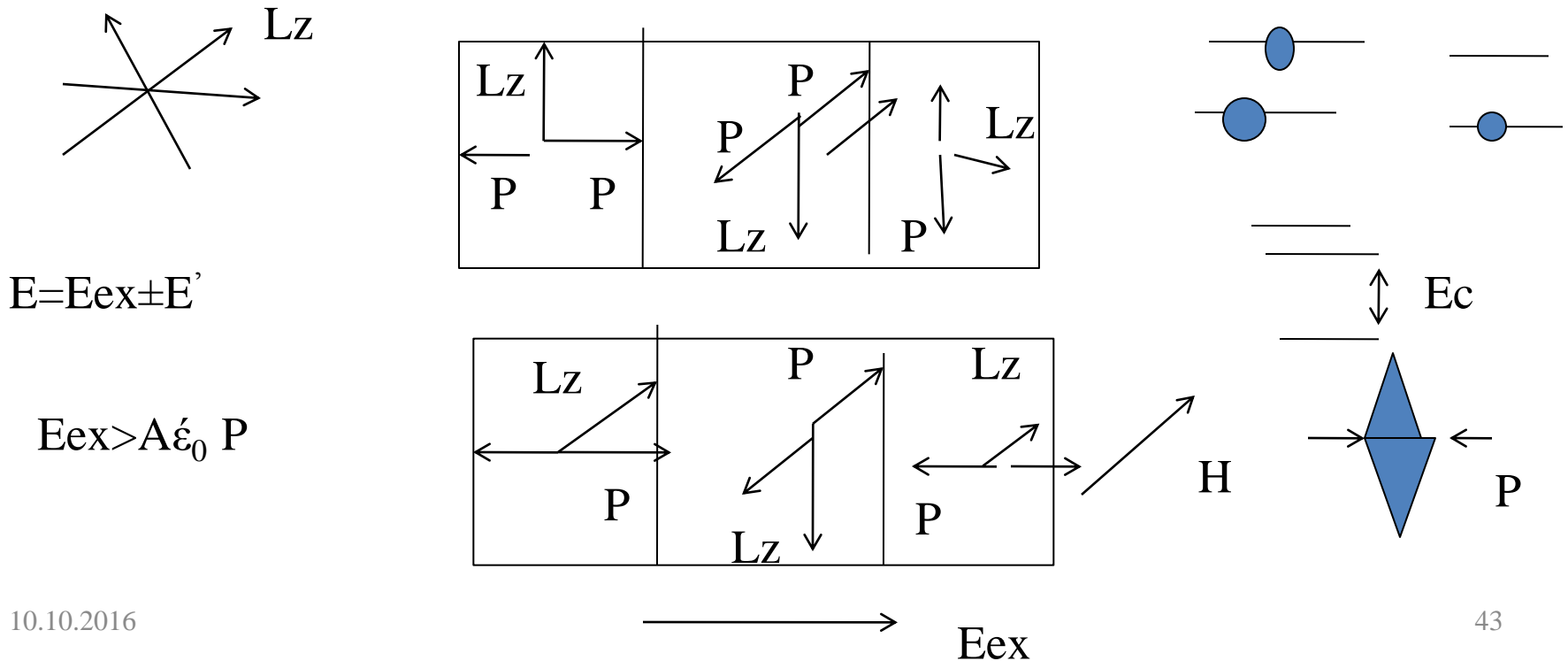


Блокировка кластеров (доменов) со случайной ориентацией орбитальных моментов

$$\frac{R(H) - R(0)}{R(0)} = \frac{u(0)}{u(H)} - 1 = A \exp(-E_{sp}/kT) - 1,$$

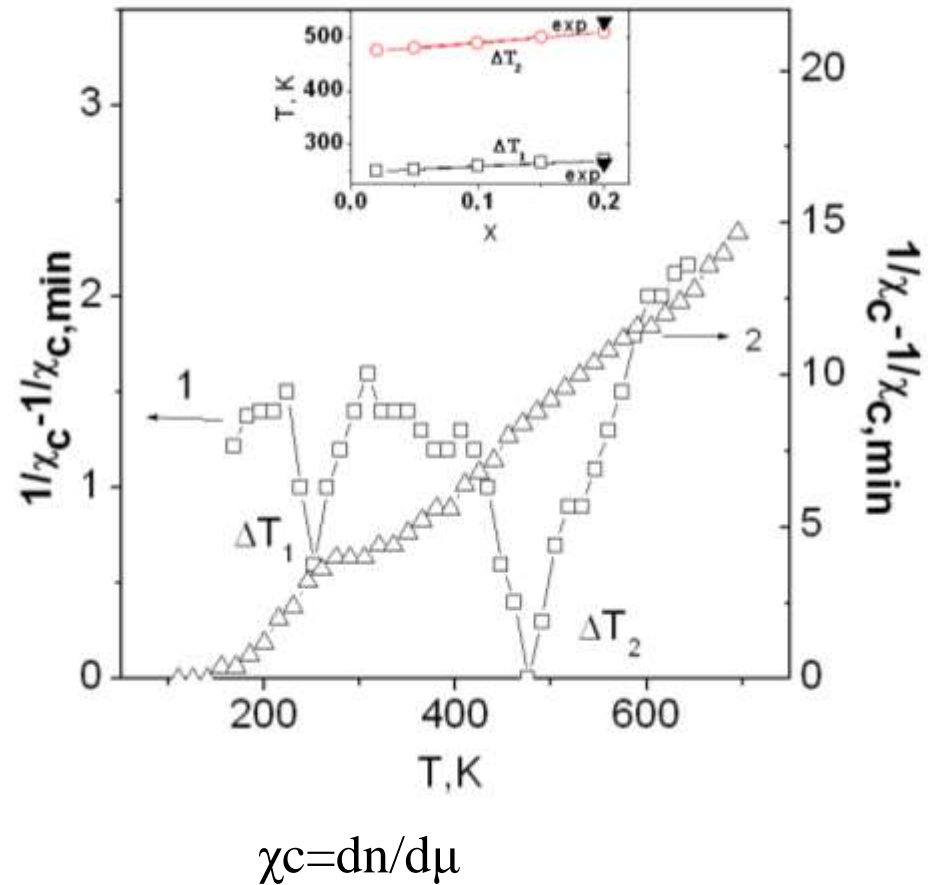
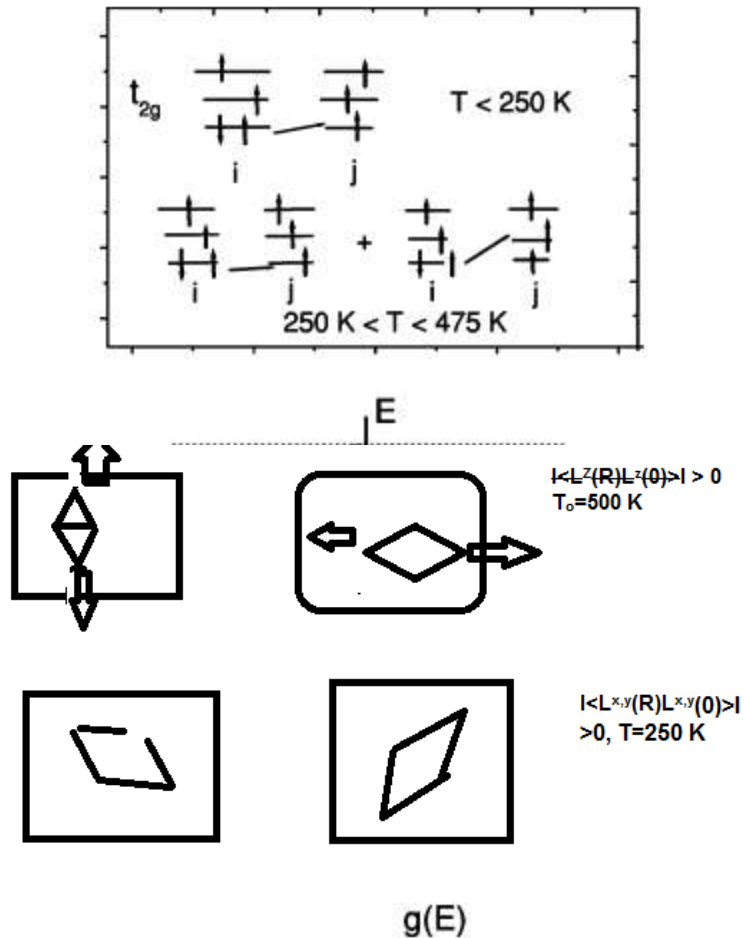
$$E_{sp} = 50 \text{ meV}, A = 9, X = 0.1; \quad E_{sp} = 3 \text{ meV}, A = 1.6, T < 320 \text{ K}$$

$$E_{sp} = 90 \text{ meV}, A = 28, T > 320 \text{ K}, \quad T > 320 \text{ K } X = 0.15$$

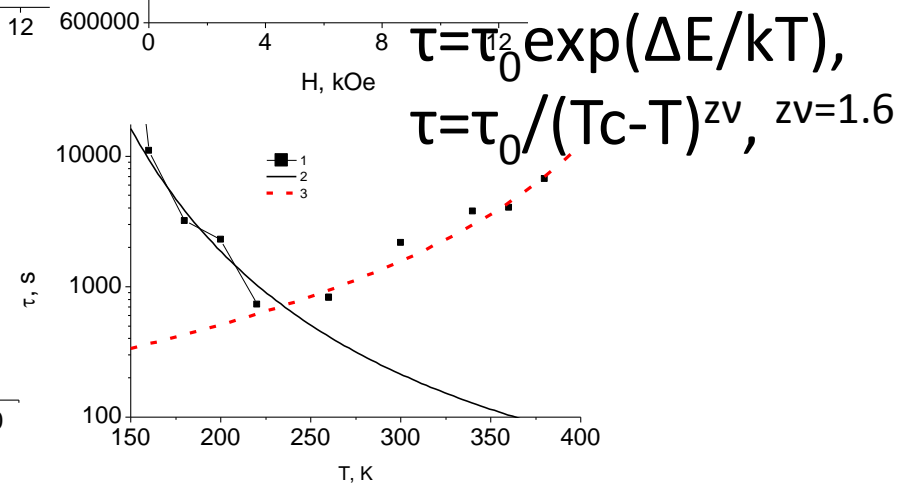
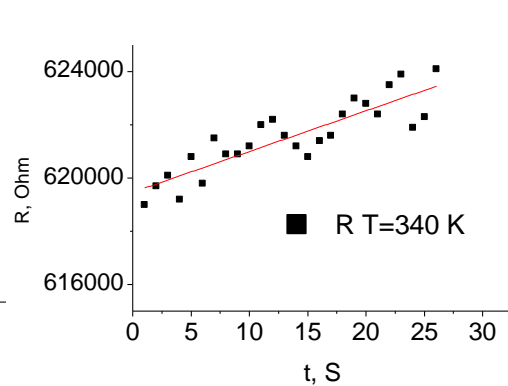
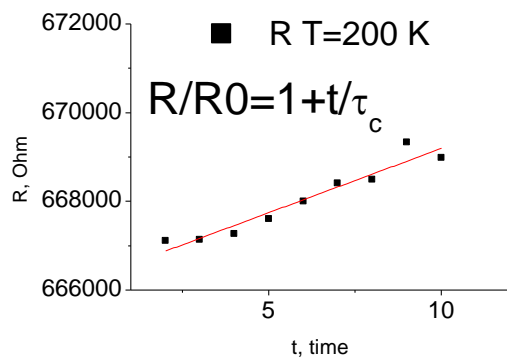
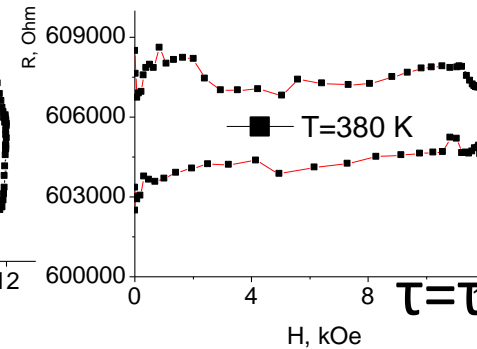
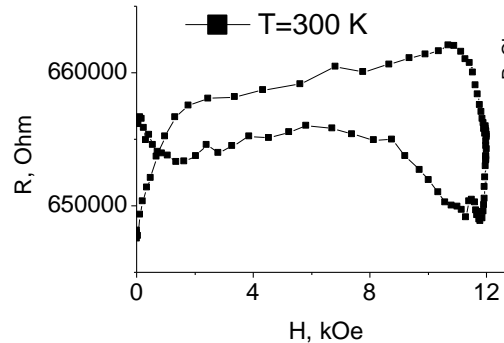
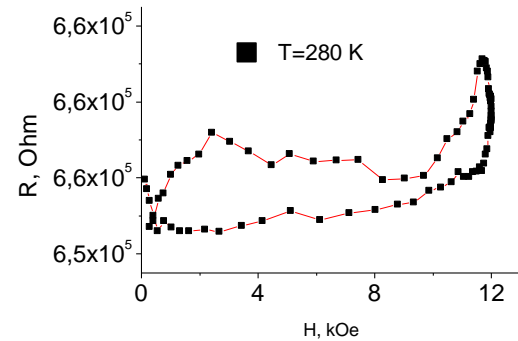
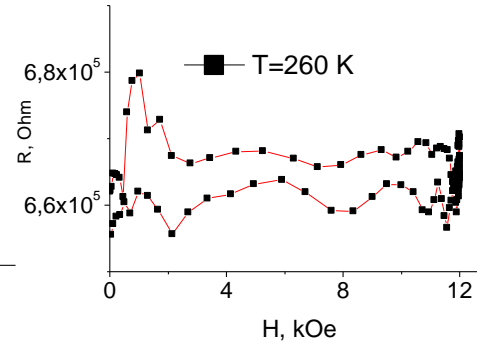
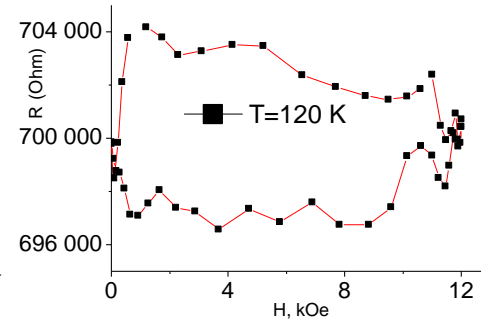
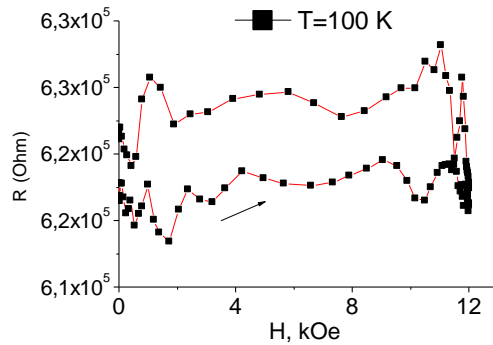


The value of the normalized charging susceptibility of electrons in t_{2g} (1) and e_g (2) bands from temperature

1 S.S. Aplesnin, L.I. Ryabinkina, G.M. Abramova et al., Phys. Rev. B **71**, 125204 (2005)



Resistance from a magnetic field in $Tm_xMn_{1-x}S$ for $x=0.1$ and annealing in the field $H=12$ kOe from time.



Resistance from a magnetic field in $Tm_xMn_{1-x}S$ for $x=0.15$ and annealing in the field $H=12$ kOe from

time

